Syntheses and Self-Assembling Characteristics of Amphiphilic Star Diblock Copolymers

Satu Strandman

Laboratory of Polymer Chemistry
Department of Chemistry
University of Helsinki
Helsinki, Finland

ACADEMIC DISSERTATION
FOR THE DEGREE OF DOCTOR OF PHILOSOPHY

To be presented, with the permission of the Faculty of Science of the University of Helsinki, for public criticism in lecture room A110, Department of Chemistry, on 14 June 2008, at 10 o'clock.

Helsinki 2008

Supervisor

Professor Heikki Tenhu
Laboratory of Polymer Chemistry
University of Helsinki
Finland

Opponent

Professor Axel H.E. Müller
Macromolecular Chemistry II
University of Bayreuth
Germany

Reviewers

Professor Ann-Christine Albertsson
Department of Polymer Technology
Royal Institute of Technology
Sweden

Professor Jukka Lukkari
Laboratory of Materials Chemistry and Chemical Analysis
University of Turku
Finland

ISBN 978-952-92-3766-1 (paperback)
ISBN 978-952-10-4665-0 (PDF)
http://ethesis.helsinki.fi
Yliopistopaino
Helsinki 2008

Abstract

Amphiphilic star diblock copolymers with hydrophobic cores and hydrophilic coronas were synthesized and their self-assembling characteristics were investigated in aqueous solutions. The number of arms in the star polymers prepared by atom transfer radical polymerization (ATRP) depended on the structure of the resorcinarene-based initiators. The structure of the initiator influenced also the rate of the polymerization of a large monomer, *tert*-butyl acrylate. Detailed NMR and molecular modeling studies suggested that the structural dependence of the initiation efficiency arises from the conformation of the macrocyclic ring. The proximity of the initiating sites increased the probability of the intramolecular coupling of radicals and thus, resulted in lower number of arms. The multifunctional initiators were employed in the preparation of four-arm and eight-arm amphiphilic star block copolymers with poly(methyl methacrylate) inner blocks and poly(acrylic acid) outer blocks.

Although amphiphilic star block copolymers have often been treated as representatives of unimolecular micelles, the current study focuses on their multimolecular assemblies in solution. Depending on the solution conditions and more importantly, on the number of arms, amphiphilic stars formed spherical or cylindrical micelle-like aggregates, or both. The morphologies of the self-assemblies were investigated by light scattering and cryo-transmission electron microscopy (cryoTEM). Star polymers with low number of arms (4) were capable of associating into wormlike micelles upon screening the charges by the addition of salt. At high pH, the wormlike species disintegrated into spherical micelles due to a higher degree of ionization of polyelectrolyte blocks and swelling of the corona owing to the higher osmotic pressure by trapped counterions. In salt-free solutions, four-arm stars also exhibited time-dependent gelation at high polymer concentrations due to the formation of a physical network by hydrophobic interactions or to the interpenetration of coronal layers of the micelle-like aggregates. Stars with high number of arms (8) formed spherical micelles in aqueous solutions: cylindrical aggregates were not observed due to higher stretching of core-forming blocks as well as higher repulsion between the polyelectrolyte blocks in the corona compared to the four-arm analogues. The results on the association behavior of amphiphilic stars were supported by computer simulations.

Acknowledgements

The current work has been carried out at the Laboratory of Polymer Chemistry, University of Helsinki under the supervision of Professor Heikki Tenhu. The work was financed by ESPOM (Electrochemical Science and Technology of Polymers and Membranes including Biomembranes) and NANO (National Graduate School in Nanoscience) graduate schools, which is gratefully acknowledged.

I wish to express my deepest gratitude to my supervisor and mentor Professor Heikki Tenhu for his continuous support, encouragement, and forbearing guidance. I am greatly indebted for his wisdom, enthusiasm, and inspiration that have lightened up my path in science. I also wish to thank him for spreading friendly and caring atmosphere to the Lab and thus, making it a pleasant place to work at.

I wish to thank my colleagues and dear friends, Dr. Sami Hietala and Dr. Vladimir Aseyev for their contribution, for sharing their time and ideas, and for their warm friendship.

I also wish to thank the following colleagues and collaborators who have contributed this work: Dr. Anna Zarembo, Professor Anatoly Darinskii and Phil.Lic. Satu Niemelä for providing the computer simulations and molecular models as well as for several fruitful discussions in the pursuit of combining the experiments and theory; Petri Pulkkinen, Dr. Minna Luostarinen and Professor Kari Rissanen for their share in the synthetic work; Dr. Sarah Butcher, Benita Löflund (Koli), and Pasi Laurinmäki for cryoTEM; Markus Nuopponen for his help with MALDI-TOF as well as for many helpful discussions on polymer synthesis; and Dr. Elina Vuorimaa-Laukkanen and Professor Helge Lemmetyinen for their help and comments on the fluorescence measurements.

Many thanks to Professor Walter Burchard, Professor Søren Hvilsted, Dr. Katja Jankova, Professor Eva Malmström, Professor Filip Du Prez, and Dr. Tilo Krause for helpful discussions and inspiration for the current work.

I wish to thank each and every one of the former and current Lab members for creating such a pleasant and innovative working atmosphere. My special thanks go to Dr. Susanna Holappa, Dr. Janne Raula, Dr. Antti Laukkanen and Dr. Jun Shan, as well as to Szymon Wiktorowicz.

Finally, I would like to thank my family, and especially my sister Johanna, for love and support. To them I dedicate this thesis.

Helsinki, 2008

Satu Strandman

Abbreviations

4HP	4-(dicyanomethylene)-2-methyl-6-(*p*-dimethylaminostyryl)-4*H*-pyran (also known as DCM)
ATRP	atom transfer radical polymerization
2,2'-bipy	2,2'-bipyridine
COSY	correlation NMR spectroscopy
cac	critical aggregation concentration
cmc	critical micellization concentration
cryoTEM	cryo-transmission electron microscopy
dNbpy	4,4'-dinonyl-2,2'-bipyridine
DEPT	distortionless enhancement by polarization transfer
DLS	dynamic light scattering
ESI-TOF	electrospray ionization time-of-flight mass spectrometry
FT-IR	Fourier transform infrared spectroscopy
HSQC	heteronuclear single quantum correlation spectroscopy
HMTETA	1,1,4,7,10,10-hexamethyltriethylenetetramine
MALDI-TOF	matrix assisted laser desorption/ionization time-of-flight mass spectrometry
NMP	nitroxide-mediated polymerization
N/A	not available
NMR	nuclear magnetic resonance spectroscopy
NOESY	nuclear Overhauser effect spectroscopy
PAA	poly(acrylic acid)
PDI	polydispersity index
PDMA	poly(N,N-dimethylacrylamide)
PEG	poly(ethylene glycol)
PMDETA	N, N',N'',N''-pentamethyldiethylenediamine
PMMA	poly(methyl methacrylate)
$(PMMA\text{-}b\text{-}PAA)_n$	poly(methyl methacrylate)-block-poly(acrylic acid), star polymer with *n* arms
$(PMMA\text{-}b\text{-}PtBA)_n$	poly(methyl methacrylate)-block-poly(*tert*-butyl acrylate), star polymer with *n* arms
PtBA	poly(*tert*-butyl acrylate)
RAFT	reversible addition-fragmentation chain transfer
RI	refractive index
ROESY	rotating-frame nuclear Overhauser effect/enhancement spectroscopy
SEC	size exclusion chromatography
SLS	static light scattering
THF	tetrahydrofuran
Et_3N	triethylamine
TFA	trifluoroacetic acid
Me_6TREN	tris(2-dimethylaminoethyl)amine

Symbols

N_{agg}	aggregation number
ω	angular frequency
q	amplitude of the scattering vector
$G_2(t)$	autocorrelation function of scattered light intensity
$G_1(t)$	correlation function of electric field
c*	critical overlap concentration
α	degree of ionization
D_θ	diffusion coefficient
f	functionality (= number of arms) of the star polymer
T_g	glass transition temperature
R_h	hydrodynamic radius
a_0	interfacial area per molecule
N_A, N_B	number of repeating units of blocks A and B
Z_0	local packing parameter at core/corona interface
G''	loss modulus
M_n/M_w	molar mass distribution (polydispersity)
ν_0	molar volume
M_n	number-average molar mass
p	packing parameter (also known as shape factor)
P(q)	particle scattering function
R_g	radius of gyration
n_0	refractive index of the solvent
η_{rel}	relative viscosity
Γ	relaxation rate
τ	relaxation time
μ_2	second cumulant
G'	storage modulus
R_{theor}	theoretical maximum radius
η_0	viscosity at zero shear rate
η_s	viscosity of the solvent
λ_0	wavelength in vacuum
M_w	weight-average molar mass

List of original publications

This thesis is based on the following publications:

I Strandman, S., Luostarinen, M., Niemelä, S., Rissanen, K., Tenhu, H. **Resorcinarene-Based ATRP Initiators for Star Polymers**. *Journal of Polymer Science Part A: Polymer Chemistry* **2004**, *42*, 4189-4201.

II Strandman, S., Pulkkinen, P., Tenhu, H. **Effect of Ligand on the Synthesis of Star Polymers by Resorcinarene-Based ATRP Initiators**. *Journal of Polymer Science Part A: Polymer Chemistry* **2005**, *43*, 3349-3358.

III Strandman, S., Hietala, S., Aseyev, V., Koli, B., Butcher, S.J., Tenhu, H. **Supramolecular Assemblies of Amphiphilic PMMA-*b*-PAA Stars in Aqueous Solutions**. *Polymer* **2006**, *47(19)*, 6524-6535.

IV Strandman, S., Tenhu, H. **Star Polymers Synthesised with Flexible Resorcinarene-derived ATRP Initiators**. *Polymer* **2007**, *48(14)*, 3938-3951.

V Strandman, S., Zarembo, A., Darinskii, A.A., Löflund, B., Butcher, S.J., Tenhu, H. **Self-assembling of star-like amphiphilic block copolymers. Effect of pH**. *Polymer* **2007**, *48(24)*, 7008-7016.

VI Strandman, S., Zarembo, A., Darinskii, A.A., Laurinmäki, P., Butcher, S.J., Vuorimaa, E., Lemmetyinen, H., Tenhu, H. **The effect of the number of arms on the association of amphiphilic star block copolymers.** *Macromolecules* submitted

The publications are referred to in the text by their Roman numerals.

Author's Contribution to the Publications

For publications I-IV, S. Strandman has independently drawn up the research plan and written the manuscripts. For publications V-VI, S. Strandman has independently drawn up the research plan and written the manuscripts in a close collaboration with Dr. A. Zarembo, who conducted the computer simulations.

Contents

ABSTRACT ..... **III**

ACKNOWLEDGEMENTS ..... **IV**

ABBREVIATIONS ..... **V**

SYMBOLS ..... **VI**

LIST OF ORIGINAL PUBLICATIONS ..... **VII**

1. INTRODUCTION **1**

1.1. REVIEW 2

1.1.1. Star polymers *2*

1.1.2. Synthetic strategies for star polymers *3*

1.1.3. Self-assembling of amphiphilic block copolymers *4*

1.2. OBJECTIVES OF THE STUDY 5

2. EXPERIMENTAL **6**

2.1. SYNTHESES OF MULTIFUNCTIONAL INITIATORS 6

2.1.1. Short note on the nomenclature *6*

2.1.2. Syntheses of resorcinarene-derived initiators[I] *6*

2.1.3. Syntheses of resorcinarene-derived initiators with a spacer[IV] *7*

2.2. POLYMERIZATIONS 8

2.2.1. Starlike homopolymers[I-IV, VI] *and block copolymers*[I, III, VI] *8*

2.2.2. Amphiphilic star block copolymers[III, VI] *9*

2.3. CHARACTERIZATION 11

3. RESULTS AND DISCUSSION **12**

3.1. RESORCINARENE-BASED INITIATORS IN THE SYNTHESIS OF STAR POLYMERS[I,II, IV] 12

3.1.1. Characteristics of the initiators *12*

3.1.2. Syntheses of star polymers. *13*

3.1.2.1. Polymerization conditions 13

3.1.2.2. Results of the polymerizations 14

3.2. SELF-ASSEMBLING OF AMPHIPHILIC STAR BLOCK COPOLYMERS[III, V, VI] 17

3.2.1. Properties of the amphiphiles *17*

3.2.2. Four-arm stars in aqueous solutions[III, V] *18*

3.2.2.1. Salt-free solutions[III] 18

3.2.2.2. Saline solutions[III, V] 19

3.2.3. Eight-arm stars in aqueous solutions[VI] *26*

4. CONCLUSIONS **32**

5. APPENDIX **34**

6. REFERENCES **35**

1. Introduction

New and emerging technologies based on polymeric materials have increased the demand for more advanced, tailor-made polymers. The synthesis of well-defined polymers and complex polymer architectures has been greatly facilitated due to the recent developments in controlled radical polymerization techniques, which has opened up new possibilities also in the design and preparation of functional nanostructures based on the supramolecular assembly. In nature, numerous structures of varying complexity can be produced upon the self-assembling of individual molecules, such as lipids and proteins, by noncovalent interactions.[1-3] Such molecules are often amphiphilic, i.e. they consist of both hydrophilic and hydrophobic moieties. Hence, an important class of synthetic polymers possessing similar self-assembling characteristics is amphiphilic block copolymers.

Amphiphilic block copolymers are composed of covalently linked hydrophilic and hydrophobic polymer chains, leading to characteristic solution properties. In block selective solvents, these polymers tend to associate to micelle-like aggregates of various morphologies, which can transform from one to another when the solution conditions are changed.[4,5] Depending on the morphology, the potential applications of the self-assemblies lie in various fields of nanotechnology, for example, in the preparation of nanoparticles of different shapes or in templating of inorganic structures for nanomaterials[6,7], as well as in the encapsulation and delivery of compounds like drugs, dyes, anticorrosion agents, flavors, and fragrances.[8-10] Amphiphilic block copolymers have also been investigated for industrial applications as rheology modifiers[11], emulsifiers[12,13], stabilizing agents of latexes[14-16] or flocculants.[17]

The most commonly utilized amphiphilic block copolymers are linear ones, but recently the research has been directed towards more complex architectures, such as starlike or graft copolymers. Such polymers may exist in aqueous solutions in their self-assembled form but also as single molecules, so called unimolecular micelles[18,19] having a core-shell structure even at low polymer concentrations, which makes them particularly attractive for solubilizing or binding hydrophobic compounds. The term ‘unimolecular micelle’ could in fact describe the structure of starlike amphiphilic block copolymers, which consist of linear block copolymers tethered to one point. Understanding the association processes is vital for controlling the self-assembling behavior of various polymer architectures. Thus, the current work focuses on investigating the self-assembling characteristics of well-defined amphiphilic star polymers both experimentally and by computer simulations.

1.1. Review

1.1.1. Star polymers

Starlike polymers exhibit a class of soft materials possessing properties intermediate between the linear polymers and colloidal suspensions.[20] Representing the most elementary case of branched polymer structures with a single branching point, they have been employed as models for the experimental evaluation of theories on the solution behavior of branched polymers[21] or on the dynamics of polymer chains tethered on curved surfaces.[20,22] They possess lower hydrodynamic volumes and different intrinsic viscosities compared with their linear counterparts, depending on the number and length (molar mass) of the arms. According to a well-established model by Daoud and Cotton[23], star polymers consist of a dense core and a soft corona, in which the arms are capable of interpenetration at semidilute solutions.[24-26] Hence, the stars with a low number of long arms approach the solution behavior of linear polymers while the ones with a high number of short arms resemble hard spheres. Highly branched macromolecules like dendrimers of higher generations exhibit "ball-bearing-like" behavior, in which the melt viscosity is not dominated by entanglements but by interdigitation.[27]

Similar to dendrimers, star polymers allow the incorporation of a large number of functional groups both in the chain ends and within the star. Examples of such functionalities are chromophores[28,29], catalytic groups[28], drugs[30], bioactive groups[31,32], as well as donor and acceptor groups for supramolecular interactions.[28] For instance, starlike poly(N,N-dimethylacrylamide) (PDMA) with L-tyrosine end groups has been successfully employed as a recyclable multifunctional chiral auxiliary for the catalytic alkylation of benzaldehyde with diethylzinc.[28] The high number of end groups also permits the crosslinking reactions and binding the stars to the surfaces. These features have been utilized, for example, in the preparation of surface-immobilized coatings of crosslinked isocyanate-terminated poly(ethylene glycol) (PEG) stars, which have been functionalized to recognize specific biomolecules like streptavidin, histidine-tagged proteins, amino-terminated oligonucleotides, and cell receptors.[32] The high crosslinking density along with the dense core of the PEG stars inhibits efficiently the adsorption of proteins onto the surfaces.[32,33]

Polymers with starlike or branched architectures have been considered as rheology modifiers with higher shear stability compared with their linear analogues, as the sacrificial scission of the branches leads only to a small decrease in molar mass.[34] The use of star polymers as porogens has also been reported for the preparation of nanoporous organosilicate insulators with ultra-low dielectric constant required in microelectronic devices.[35] To summarize, the potential of star polymers lies both in their shape and their functionalities.

1.1.2. Synthetic strategies for star polymers

Previously, starlike polymers have been prepared by synthetically demanding living ionic procedures, which have poor compatibility with functional groups.[36,37] During the past decade, several controlled radical polymerization techniques have been developed to overcome these limitations. The basic synthetic strategies for starlike polymers are the arm-first and core-first approaches (Scheme 1), analogous to the convergent and divergent strategies for dendrimers.[38]

The arm-first approach involves the synthesis of arms that are bound together with multifunctional linking agents[36,37] or by the block copolymerization of divinyl reagents to the arms, followed by the formation of a microgel core and core-core coupling.[39,40] This approach permits the characterization of individual arms prior to the synthesis of starlike polymers. However, the removal of linear precursors is often required, and the product may consist of stars with varying number of arms, particularly if the efficiency of the linking agent is low.[41]

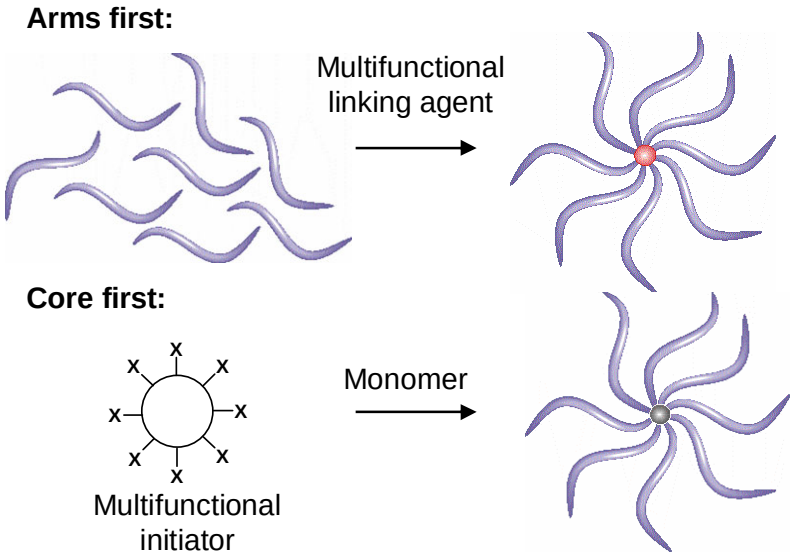

Scheme 1 *Synthetic strategies for the preparation of star polymers*

The core-first approach utilizes multifunctional initiators or transfer agents. This strategy allows the synthesis of stars with a predetermined number of arms, the functionalization of end groups, and simple chain extension.[36] Although small phenolic compounds or polyols can be employed[42-44], macrocyclic compounds or dendrimers provide a high number of functional groups to be derivatized to obtain starlike polymers. For example, cyclodextrins have been used as starting compounds for initiators and transfer agents for several controlled polymerization techniques,[45-47] and calixarene-based initiators have successfully been utilized in the synthesis of starlike polymers both by living cationic polymerization[48,49] and atom transfer radical polymerization, ATRP.[50-53] Some drawbacks of the core-first approach are the radical-radical coupling reactions

during the polymerization or lowered initiation efficiencies, both leading to deviations from the predicted number of arms.[54,55] These features will be discussed in more detail in the current thesis.

1.1.3. Self-assembling of amphiphilic block copolymers

Similar to low-molar-mass surfactants, amphiphilic block copolymers undergo micellization in block selective solvents above a certain concentration called critical micellization concentration (cmc) or critical aggregation concentration (cac). In general, polymeric micelles* exhibit the slower diffusion rates and reduced mobilities of the chains, depending on the glass transition temperature (T_g) of the core-forming blocks.[56] The advantages of amphiphilic block copolymers over the classical surfactants lie in the low critical aggregation concentration, highly tunable composition and architecture, the dependence of the micellization on selective solvents, as well as in the ability to trap unstable or metastable structures due to the slow kinetics.[57,58]

The shape and size of the self-assemblies of amphiphilic block copolymers are governed by the balance between three major forces acting on the system, reflecting the constraints between the core-forming blocks, the interaction between the chains in the corona, and the surface energy between the solvent and the core.[22] The balance between these factors depends on the structure and composition of the block copolymer, and can be perturbed by changing the properties of the solvent, or by the application of solution stimuli, such as salts, acids, bases, or surfactants,[5,58] which will often lead to a transition between the micellar morphologies. The most commonly observed morphologies are spheres, cylinders, and vesicles (Scheme 2).[1,5] In addition, a variety of other structures have been reported, including toroids[59], helices[60], disks[61], nanotubes[62], and multicompartment micelles[63]. Such complex self-assemblies have rarely been observed for classical low-molar-mass surfactants.

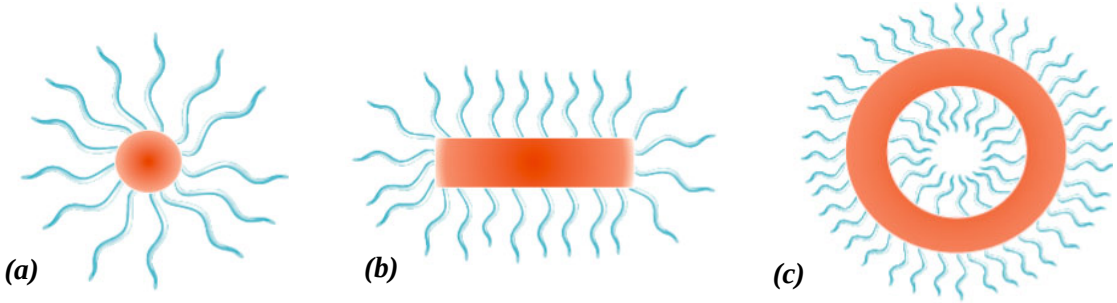

Scheme 2 *Schematic drawings of common self-assemblies of amphiphilic block copolymers in block selective solvents: (a) spherical micelle, (b) cylindrical micelle, (c) vesicle*

* *While the term 'micelle' refers to equilibrium structures, the nonequilibrium structures at $T<T_g$(core) should be called 'micelle-like aggregates'. However, the term 'micelle' is extensively used in literature and hence, it will be used here.*

1.2. Objectives of the study

The primary objective of this research was to achieve understanding about the factors affecting the self-assembling characteristics of amphiphilic star block copolymers in aqueous solutions. The syntheses of star polymers by "core-first" approach aiming at the preparation of amphiphilic star block copolymers involved the syntheses and characterization of new macrocycle-based initiators for atom transfer radical polymerization (ATRP). Therefore the overall study can be divided into two sections: the one focusing on the initiators (papers I, II, IV), and the other concentrating on the amphiphilic star block copolymers (papers III, V, VI).

The key objectives of the first section were the syntheses of resorcinarene-derived ATRP initiators with different steric properties and the investigation of the factors affecting their initiating efficiency in the preparation of starlike polymers. Two monomers with different reactivities and sizes, *tert*-butyl acrylate (tBA) and methyl methacrylate (MMA), as well as various catalysts and reaction conditions have been employed.

The goals of the second section were synthesizing amphiphilic star block copolymers and studying their self-association in aqueous solutions. The solubility in water was attained by the order and length of the blocks: the inner block of the stars was hydrophobic poly(methyl methacrylate) (PMMA) and the outer block was hydrophilic poly(acrylic acid) (PAA). The investigated variables in the self-assembling studies involved the shape (the number of arms) and composition of the stars as well as the solution conditions.

More specifically, the objectives were:

- to synthesize multifunctional resorcinarene-derived initiators, and studying their initiating properties and conformations (I)
- to clarify how the structure of the catalyst affects the initiating efficiency (II)
- to explore how the structure of the initiator influences the initiating efficiency by varying the distance of the initiating sites from the resorcinarene core by a spacer (IV)
- to investigate the self-assembling characteristics of the synthesized four-arm amphiphilic star block copolymer in aqueous solutions (III)
- to find out the effect of pH on the polymer presented in paper III both experimentally and by computer simulations (V)
- to investigate the self-assemblies of synthesized eight-arm amphiphilic star block copolymers in aqueous solutions both experimentally and by computer simulations (VI)

2. Experimental

2.1. Syntheses of multifunctional initiators

2.1.1. Short note on the nomenclature

The IUPAC names of the resorcinarenes and their derivatives will be abbreviated for simplicity. The name *'tetraethylresorcinarene'* or *'2,8,14,20-tetraethylresorcinarene'* will be used instead of 2,8,14,20-tetraethylpentacyclo[19.3.1.$1^{3,7}$.$1^{9,13}$.$1^{15,19}$]octacosa-1(25), 3(28),4,6,9(27),10,12,15(26),16,18,21,23-dodecaene-4,6,10,12,16,18,22,24-octol (*CAS 135971-85-6*), and *'tetramethylresorcinarene'* or *'2,8,14,20-tetramethylresorcinarene'* instead of 2,8,14,20-tetramethylpentacyclo[19.3.1.$1^{3,7}$.$1^{9,13}$.$1^{15,19}$]octacosa-1(25), 3(28),4,6,9(27),10,12,15(26),16,18,21,23-dodecaene-4,6,10,12,16,18,22,24-octol (*CAS 65338-98-9*). The IUPAC names of the synthesized compounds are listed in the Appendix.

2.1.2. Syntheses of resorcinarene-derived initiators[I]

Multifunctional tetraethylresorcinarene-based initiators, octakis(2-bromopropionyloxy)-tetraethylresorcinarene (**1**, *CAS 778613-19-7*) and octakis(2-bromoisobutyryloxy)tetra-ethylresorcinarene (**2**, *CAS 778613-20-0*) were prepared by adapting the method described by Angot *et al.*[51] (Scheme 3). The initiators were synthesized by the reaction of tetraethylresorcinarene (1.6 mmol) with either 2-bromopropionyl bromide (40 mmol) or 2-bromoisobutyryl bromide (40 mmol) in the presence of triethylamine (Et_3N, 40 mmol) in tetrahydrofuran (THF) at room temperature. After the filtration of precipitated $Et_3N{\cdot}HBr$ and subsequent extractions, the product was separated either by column chromatography (**1**) or by crystallization (**2**), both in the mixtures of solvents with different polarities.

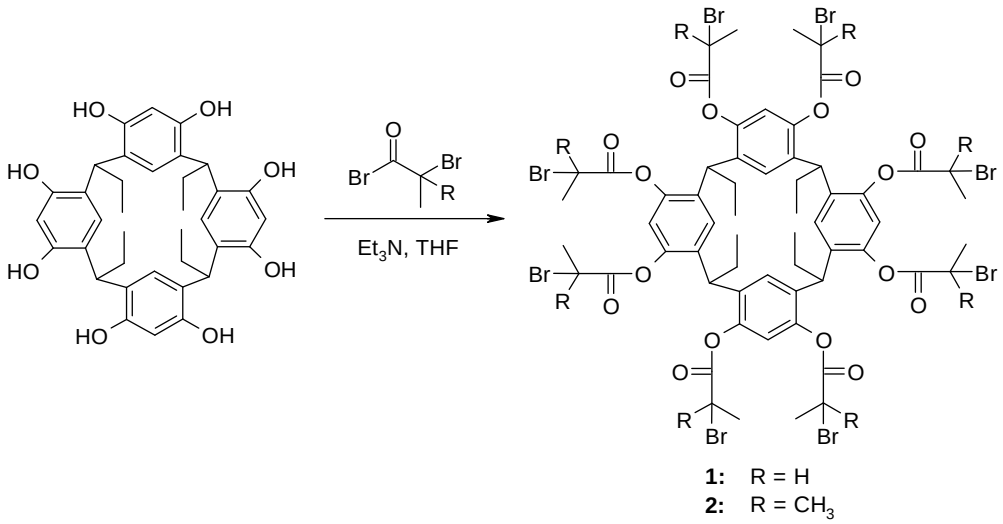

Scheme 3 *Syntheses of resorcinarene-based initiators **1** and **2***

2.1.3. Syntheses of resorcinarene-derived initiators with a spacer[IV]

Spacer-equipped multifunctional initiators, octakis(2-bromopropionylethoxy)tetramethylresorcinarene (**5**, *CAS 946502-71-2*) and octakis(2-bromoisobutyrylethoxy)tetramethylresorcinarene (**6**, *CAS 946502-72-3*) have been synthesized in the following steps (Schemes 4 and 5). First, tetramethylresorcinarene (4.6 mmol) was derivatized with ethyl bromoacetate (0.7 mol) in the Williamson ether synthesis[64] to yield compound **3**, which was crystallized from 2-propanol (Step 1). Compound **3** (4.0 mmol, *CAS 171799-35-2*) was reduced by $LiAlH_4$ (62 mmol) in dry THF to compound **4**, again crystallized from 2-propanol (Step 2).[64] The initiators were synthesized by the reaction of compound **4** (1.1 mmol, *CAS 65378-51-0*) with either 2-bromopropionyl bromide (26.8 mmol) or 2-bromoisobutyryl bromide (26.8 mmol) in the presence of triethylamine (Et_3N, 26.8 mmol) in tetrahydrofuran (THF) at room temperature (Step 3). The product was separated either by column chromatography in a mixture of petroleum ether and ethyl acetate (**5**) or by crystallization in methanol (**6**).

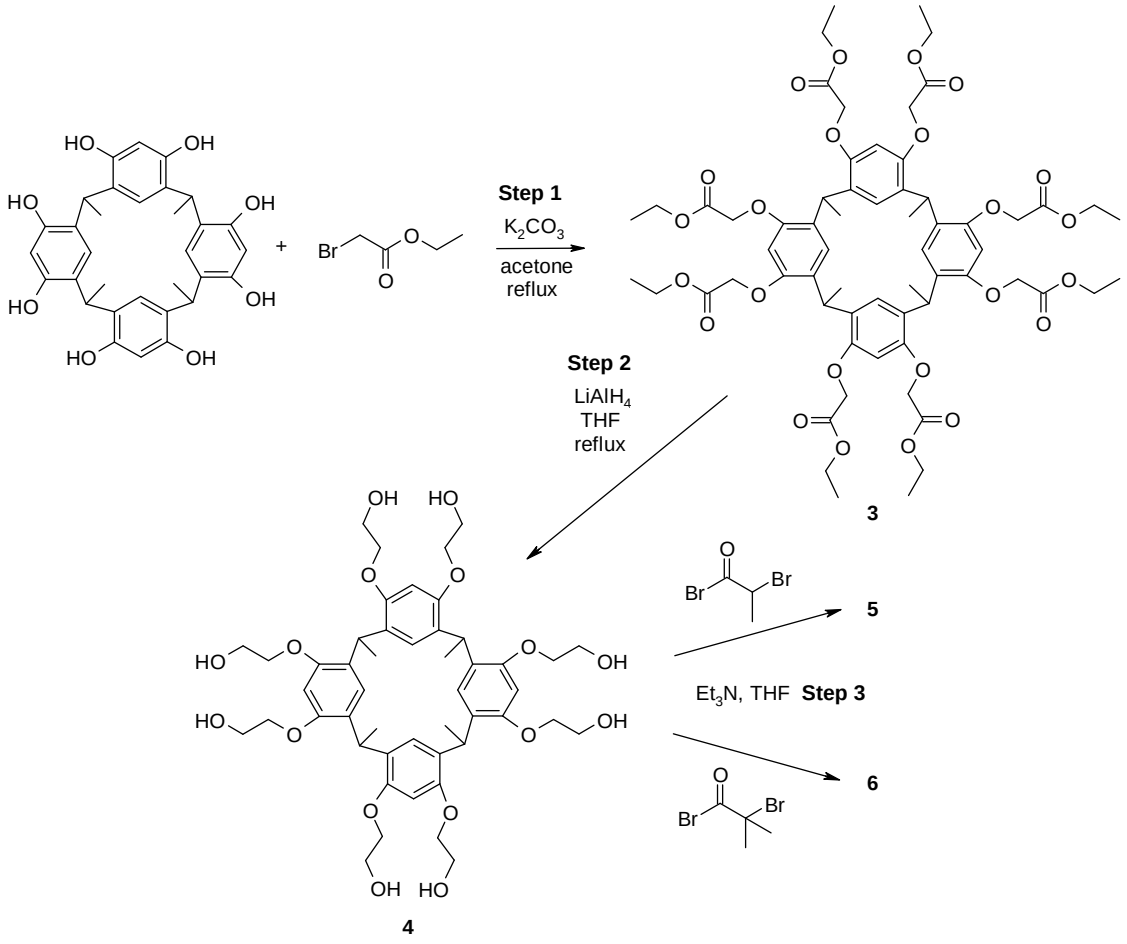

Scheme 4 *Synthesis route for the preparation of resorcinarene-derived initiators **5** and **6***

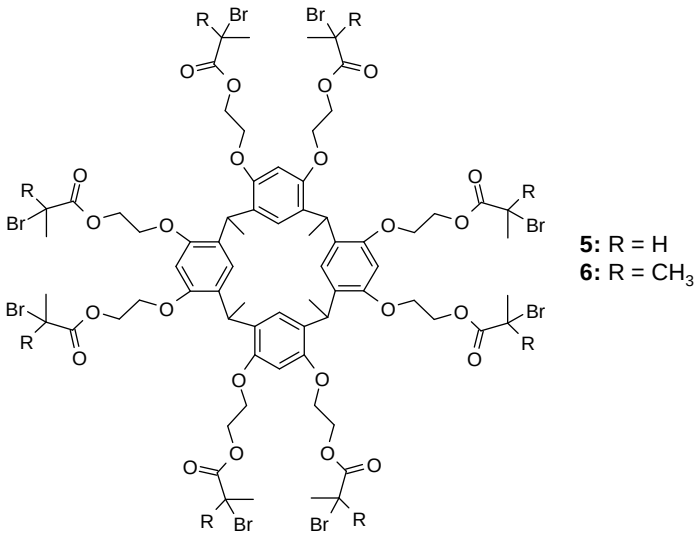

Scheme 5 *Structure of spacer-bearing resorcinarene-derived initiators **5** and **6***

2.2. Polymerizations

2.2.1. Starlike homopolymers[I-IV, VI] and block copolymers[I, III, VI]

The atom transfer radical polymerizations of *tert*-butyl acrylate (tBA) were conducted using the initiators **1** and **5**, and the polymerizations of methyl methacrylate (MMA) were conducted by the initiators **2** and **6**. The former syntheses employed CuBr catalysts and ethylene carbonate as an additive (11.4 mass %), while the latter ones were catalyzed by CuCl in various solvents (diphenyl ether, toluene, or anisole, all at 50 % of the total volume of the reaction mixture). Various ligands complexing the copper compounds (2,2'-bipy, dNbpy, PMDETA, HMTETA, Me_6TREN; Scheme 6) were utilized. The stoichiometry depended on the ligand; for 2,2'-bipy and dNbpy $[I_s]$:[CuX]:[ligand] = 1:1:2, whereas for other ligands $[I_s]$:[CuX]:[ligand] = 1:1:1. Here X = Br or Cl, and $[I_s]$ is the concentration of a single initiating group. The monomer-to-initiator ratios ([M]/[I]) were varied from [M]/[I] = 800 to 6400. The kinetic studies were conducted either by several simultaneous polymerizations taken to different conversions, or by carrying out the reaction under nitrogen atmosphere in a Schlenk tube and withdrawing small aliquots of the reaction mixture at regular intervals.

Prior to the polymerization, the reaction mixtures were degassed by the freeze-thaw method. After the reaction at 100 °C (tBA) or at 90 °C (MMA), the solutions were cooled by dipping the reaction vessel into liquid nitrogen. Copper salts were removed by passing the solution through a column packed with silica (80%) and neutral alumina (20%) in two layers. Poly(*tert*-butyl acrylates) were precipitated in a mixture of methanol and water while poly(methyl methacrylates) were precipitated in methanol.

The block copolymerizations were conducted utilizing starlike poly(*tert*-butyl acrylate) and poly(methyl methacrylates) as macroinitiators in the atom transfer radical polymerizations of methyl methacrylate and *tert*-butyl acrylate, respectively. The polymerizations took place in the same reaction conditions as the homopolymerizations. Four-arm stars were synthesized by the initiators introduced in Section 2.1.2., and eight-arm stars by those introduced in Section 2.1.3.

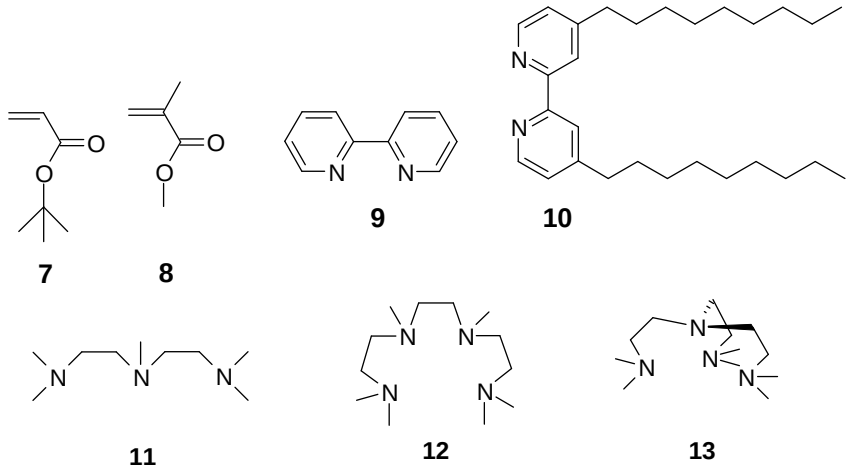

Scheme 6 *Structures of the employed monomers and ligands: (**7**) tert-butyl acrylate, (**8**), methyl methacrylate, (**9**) 2,2'-bipy, (**10**) dNbpy, (**11**) PMDETA, (**12**) HMTETA, (**13**) Me_6TREN. The synthesis of Me_6TREN is described in paper II.*

2.2.2. Amphiphilic star block copolymers[III, VI]

Amphiphilic (PMMA-*b*-PAA)$_n$ star block copolymers with poly(methyl methacrylate) core and poly(acrylic acid) shell were prepared by the hydrolysis of poly(*tert*-butyl acrylate) blocks of starlike (PMMA-*b*-PtBA)$_n$ block copolymers to poly(acrylic acid) overnight at room temperature using trifluoroacetic acid (TFA, 5 equivalents to the *tert*-butyl ester groups) in dichloromethane (CH_2Cl_2).[65] The resulting amphiphiles were purified by dialysis. The degrees of hydrolysis were estimated from ^{1}H NMR spectra in a d_6-acetone/D_2O mixture or in d_6-DMSO. The amphiphilic character of the star block copolymers was demonstrated by ^{1}H NMR spectroscopy: the resonance signals from PMMA core could not be seen in D_2O, but they appeared upon the addition of either d_6-acetone or $CDCl_3$, indicating that in water the insoluble PMMA core is hidden within the uni- or multimolecular micelles formed by (PMMA-*b*-PAA)$_n$ stars. The details of the amphiphilic star block copolymers as well as their precursors are presented in Table 1.

Entry	Polymer[a]	Conv %	M_n(theo) g/mol[b]	M_n(NMR) g/mol[c]	M_n(SEC, RI) g/mol[d]	M_w/M_n (RI)	M_n(SEC, LS) g/mol[e]	M_w/M_n (LS)
14	$(PMMA_{73})_4$	13.1	43600	26700	31100	1.3	N/A[f]	N/A
15	$(PMMA_{73}$-*b*-$PtBA_{143})_4$	19.8	112400	90200	102600	1.33	N/A[g]	N/A
16	**$(PMMA_{73}$-*b*-$PAA_{143})_4$**			**61300**	**71200**	**1.33**		
17	$(PMMA_{77})_8$	9.1	53100	63500	50500	1.15	63400	1.20
18	$(PMMA_{77}$-*b*-$PtBA_{86})_8$	11.7	159100	151400	114700	1.13	134500	1.17
19	**$(PMMA_{77}$-*b*-$PAA_{86})_8$**			**112900**			**103500**	**1.17**
20	$(PMMA_{65})_8$	8.6	50300	54000	50100	1.13	53900	1.17
21	$(PMMA_{65}$-*b*-$PtBA_{108})_8$	14.0	168800	164700	133400	1.18	142500	1.28
22	**$(PMMA_{65}$-*b*-$PAA_{108})_8$**			**116200**			**103700**	**1.28**

a) Compositions calculated from M_n(SEC, RI) or M_n(NMR);

b) M_n(theor) = [M]/[I] × conv × M(monomer) + M_n(initiator or macroinitiator) where 'conv' is for conversion;

c) By NMR analysis. M_n of $(PMMA\text{-}b\text{-}PAA)_n$ calculated from M_n(NMR) of $(PMMA\text{-}b\text{-}PtBA)_n$ assuming that the degree of hydrolysis is 100 %. The degrees of hydrolysis determined by ^1H NMR, were 98 %, 89 % and 95 % of the *tert*-butyl ester groups for entries **16**, **19**, and **22**, respectively;

d) By SEC analysis from RI signal. M_n of $(PMMA\text{-}b\text{-}PAA)_n$ as in (c), but from M_n(SEC, RI);

e) By SEC analysis from LS signal. M_n of $(PMMA\text{-}b\text{-}PAA)_n$ as in (c), but from M_n(SEC, LS);

f) M_w determined by SLS in THF, dn/dc = 0.092 mL/g: M_w(SLS) = 88800 g/mol;

g) M_w determined by SLS in THF, dn/dc = -0.032 mL/g: M_w(SLS) = 400000 g/mol

2.3. Characterization

The composition and structure of multifunctional initiators[I, IV] has been determined by FT-IR spectroscopy, elemental analysis (by Analytische Laboratorien GmbH, Lindlar, Germany), mass spectrometry (ESI-TOF or MALDI-TOF), as well as by various NMR techniques: ^{1}H and ^{13}C NMR, DEPT, COSY, HSQC, and ROESY. The last technique was utilized in the conformational studies of the initiators.[I] The conformational studies involved also molecular modeling by InsightII and Discover molecular modeling packages from Accelrys Inc.[I]

The conversions of the polymerizations were determined from the reaction mixtures by ^{1}H NMR. The polymers were characterized by size exclusion chromatography (SEC), ^{1}H and ^{13}C NMR, FT-IR and in some cases, by static light scattering (SLS).[I, II, IV] The numbers of arms (*f*) in the starlike homopolymers were determined by the alkaline cleavage of the arms followed by the SEC analysis[I, II, IV], and by ^{1}H NMR analysis of the polymers.[IV]

The self-assembling characteristics of amphiphilic star block copolymers in aqueous solutions were probed by dynamic and static light scattering (DLS, SLS) [III, V, VI] as well as by rheometry.[III] The former methods were employed for investigating the hydrodynamic sizes and structures of self-assembled 4-arm and 8-arm amphiphilic stars in salt-containing solutions, while the latter technique was utilized for studying the viscoelastic properties of the salt-free solutions of the 4-arm star polymer. The critical aggregation concentrations (cac) of the 8-arm amphiphiles were determined by steady-state fluorescence spectrometry as well as by light scattering.[VI] The shapes of the self-assemblies were ascertained by direct imaging of the solutions by cryo-transmission electron microscopy (cryoTEM).[III, V, VI]

In parallel with the experiments, the self-assembling behavior of both 4-arm and 8-arm amphiphilic star block copolymers in various solution conditions was explored by coarse-grain computer simulations.[V,VI]

3. Results and discussion

3.1. Resorcinarene-based initiators in the synthesis of star polymers[I,II, IV]

3.1.1. Characteristics of the initiators

Most of the ATRP initiators for the preparation of star polymers are based on multifunctional inorganic or organic compounds bearing halogen groups or hydroxyls that can be converted to chloro- or bromoesters. In the current work, macrocyclic compounds bearing eight (8) hydroxyl groups, resorcinarenes, have been successfully derivatized to two types of multifunctional initiators, rigid and flexible ones (Schemes 3 and 5). Like calixarenes, resorcinarenes carry a circular array of hydrogen bonds between the phenolic hydroxyl groups which breaks upon the derivatization, altering the conformational and complexing properties of the macrocycle.[66-68] The parent compounds, tetraethyl-resorcinarene and tetramethylresorcinarene, are both all-*cis* conformers holding all four ethyl or methyl groups in the axial position. As the conformers are designated according to the positions of the substituents in the methine bridges (*cis c*, *trans t*) relative to the reference group, the all-*cis* conformer is designated as *rccc* (Scheme 7).[69]

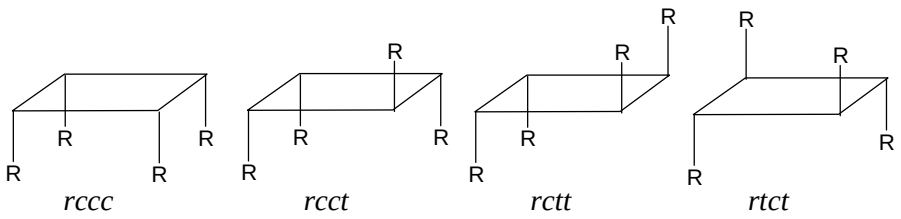

Scheme 7 *Orientations of the substituents in methine bridges of resorcinarenes*[69]

The principal arrangements which the resorcinarene ring itself may adopt are the *crown* (C_{4v}), *boat* (C_{2v}), *chair* (C_{2h})[69], *diamond* (C_s)[70], and *saddle* (D_{2d})[69] conformations (Scheme 8). According to ^1H and ^{13}C NMR spectra,[I, IV] both parent compounds possess symmetric *crown* (C_{4v}) conformations prior to the derivatization. It has been shown experimentally that the *rccc* isomer can exist in both *crown* and *boat* conformations.[71,72] If the rate of conformational interconversion is high, only the signals of *crown* conformation are visible in the NMR spectra.[70]

The acylation of tetraethylresorcinarene yielding initiators **1** and **2** led to slower interconversion due to the breakage of stabilizing hydrogen bonds. Therefore, the NMR spectra of **1** and **2** indicated that these compounds adopt a C_2-symmetric *boat* conformation in which aromatic groups lie spatially in pairs.[I] Slower conformational

interchange was also observed upon the preparation of flexible initiators **5** and **6** by the derivatization of tetramethylresorcinarene, first by the etherification of phenolic groups (Step 1 in the Section 2.1.3.), followed by the reduction of the substituents (Step 2), and the acylation (Step 3). Like their rigid counterparts, the resulting initiators **5** and **6** adopt a *boat* conformation (C_{2v}).[I] The polymerization studies by the initiators led to more detailed conformational investigations, which both will be described in Section 3.1.2.2.

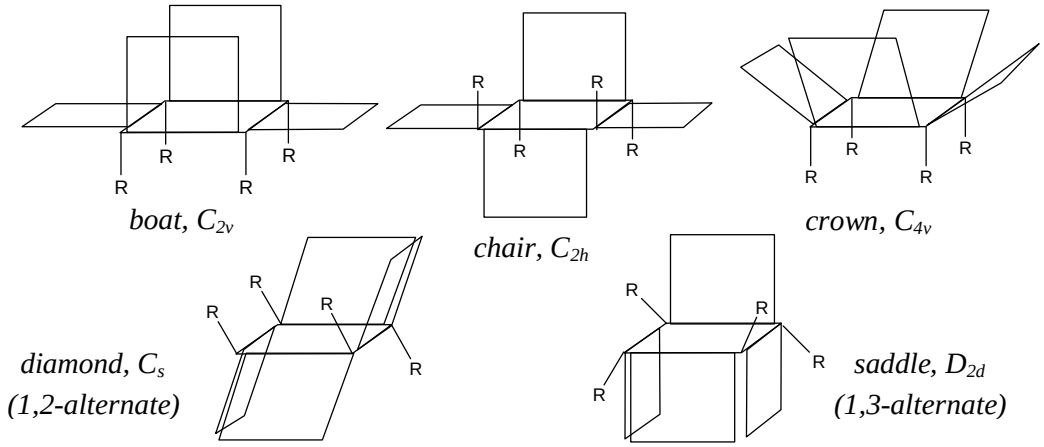

Scheme 8 *Possible conformers of resorcinarenes*

3.1.2. Syntheses of star polymers

3.1.2.1. Polymerization conditions

The monomers employed for the polymerizations were *tert*-butyl acrylate, tBA (**7**), and methyl methacrylate, MMA (**8**). The reactivities and sizes of these monomers are different and moreover, poly(*tert*-butyl acrylate) is commonly utilized as a precursor for hydrophilic poly(acrylic acid) via acidic or thermal cleavage of *tert*-butyl ester groups.[65, 73] Therefore, these monomers also serve as building blocks for the preparation of amphiphilic polymers. The initiating sites should mimic the growing polymer chains.[74] Hence for studying the initiation activities as well as the polymerization kinetics, the initiators **1** and **5** with 2-bromopropionyl groups were used to polymerize tBA, and the initiators **2** and **6** with 2-bromoisobutyryl groups were used in the polymerization of methyl methacrylate, MMA, due to their higher rate of activation.[74.75] The control over the polymerization of tBA in bulk was improved by the addition of a polar compound, ethylene carbonate[51], while the polymerization of MMA in solution was enhanced by the halogen exchange, that is, the polymerization by the bromine-containing initiator has been catalyzed by CuCl.[76]

The electronic and steric properties of the ligand have a strong influence on the activity of the catalyst and the control over the polymerization.[77,78] In the activation process of ATRP (Scheme 9), the transition metal complex (Mt^nLY) cleaves homolytically the carbon-halogen bond of the initiating or dormant species (R-X or P_m-X) to generate a metal complex with a higher oxidation state ($XMt^{n+1}LY$) and a carbon-centered radical (R· or P_m·), which then adds to the monomer (M). In the reverse deactivation process, the dormant species (P_m-X) is formed again. An ideal catalyst should provide an appropriate rate of activation and fast deactivation.[78] Bulky ligands, for instance 2,2'-bipy (**9**) and dNbpy (**10**), reduce the accessibility of the transition metal by halogen, decreasing the rate of activation.[79] Replacing the bipyridine with smaller multidentate amines, such as PMDETA (**11**), HMTETA (**12**), or Me_6TREN (**13**), will reduce the steric hindrance by the initiating sites and increase the rate of polymerization.[80] Hence, systematic studies on the effect of various catalysts on the polymerization kinetics as well as on the functionalities of the stars were conducted.

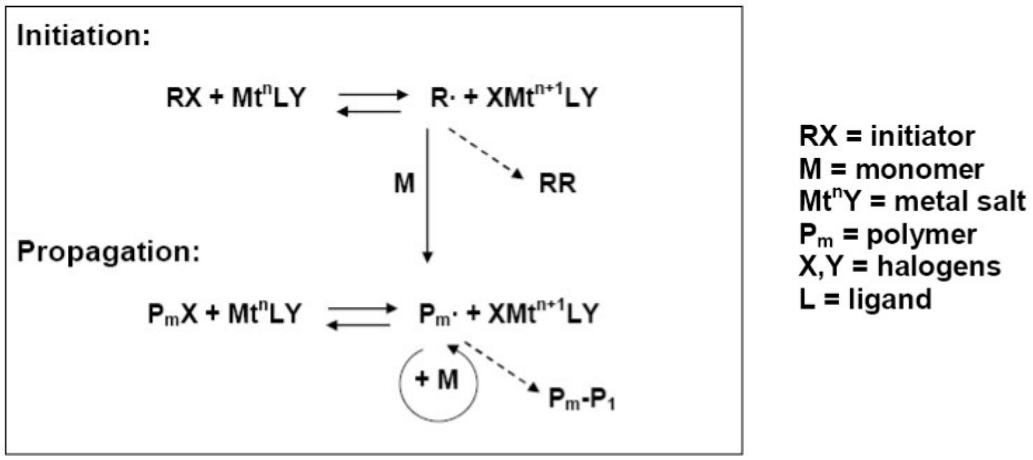

Scheme 9 *Mechanism of atom transfer radical polymerization, ATRP*[81]

3.1.2.2. Results of the polymerizations

The major difference between the rigid (**1**,**2**) and flexible (**5**,**6**) resorcinarene-based initiators lies in the functionalities (the number of arms, *f*) of the stars they produce. According to the SEC analyses of the stars and their detached arms, the rigid initiators yielded stars with $f \sim 4$, irrespective of the chosen catalyst[I, II], whereas the flexible initiators produced stars with higher average functionalities, $f \sim 6$ by **5** (PtBA) and $f \sim 7$ by **6** (PMMA).[IV] The latter results were obtained both by SEC and by NMR, owing to the visible signals from the large initiators. The difference between the functionalities of PtBA and PMMA stars in the latter case may stem from the bulky structure of *tert*-butyl acrylate, or from the higher dilution of methyl methacrylate, decreasing the number of propagation events that occur before the deactivation of the radicals.[82]

Detailed conformational studies of the initiators by ROESY NMR and molecular modeling suggest that the four out of eight initiating sites of the rigid initiators are in proximity to each other in the dominant *boat* conformation (Figure 1)[I], while the initiating sites of the flexible initiators keep further apart because of the spacers.[IV] Therefore, lower functionalities of the stars may stem from the intramolecular coupling of radicals due to the steric hindrance of the initiators, arising both from their structure and conformation.[I,IV] In highly flexible systems, intramolecular cyclization has also been observed due to the backfolding of initiating end groups.[82-84] Steric hindrance of the initiator or the catalyst plays an important role particularly in multifunctional initiating systems, such as dendrimer-based initiators and brush-like macroinitiators.[55, 82-88]

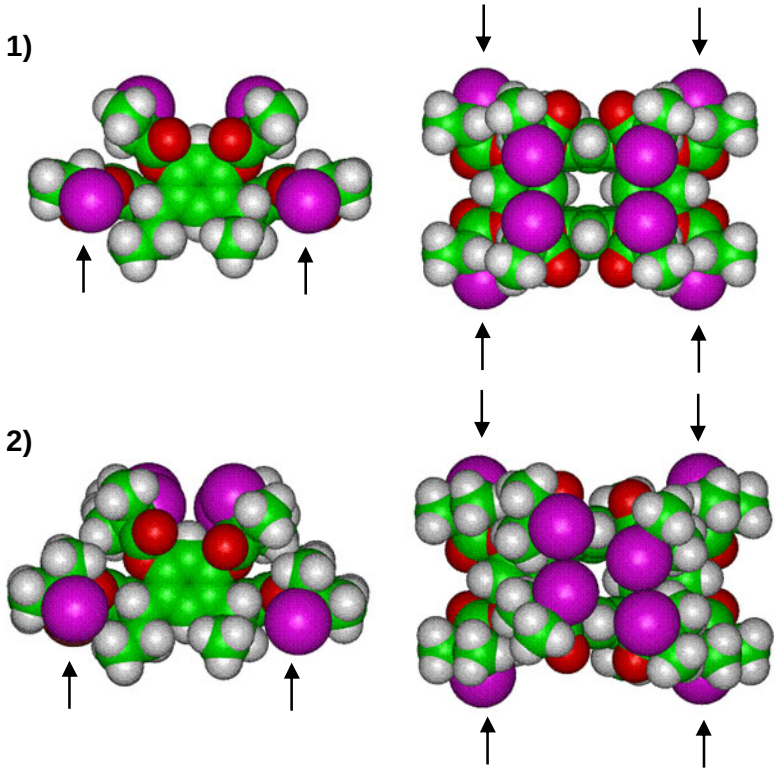

Figure 1 *Side (left) and top (right) views of the space-filling models of initiators **1** and **2** in a boat conformation. Conformations correspond to one of the local minimum conformations. The arrows indicate the active initiating sites.*

Another difference between the initiators was observed in the kinetics of the polymerizations.[IV] The flexible initiator (**1**) provided faster polymerization of tBA than the rigid one (**5**) (Figure 2). This refers to lower steric hindrance that increases the efficiency of initiating sites during the polymerization of bulky *tert*-butyl acrylate monomer. The higher number of growing chains increases also the rate of polymerization.[41] The apparent polydispersities were lower by the flexible initiator, indicating more controlled polymerization or, as shown above, higher number of arms. According to Flory[89], the polydispersities of stars consisting of arms with 'the most probable distribution' of chain lengths depend on the number of arms (*f*):

(1) $M_w/M_n = 1 + (1/f)$

The structure of the initiator had little effect on the polymerization kinetics of MMA, possibly due to a very fast and less controlled polymerization (Figure 3).

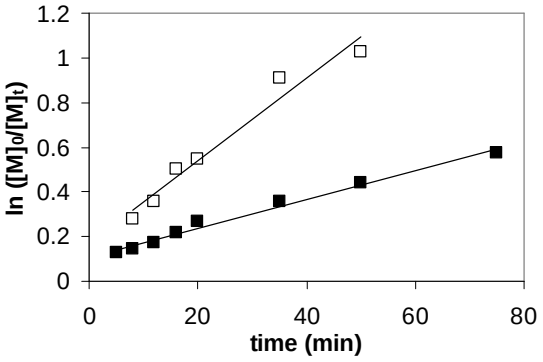

Figure 2 *Kinetic plot of monomer conversion as a function of reaction time for the polymerization of tert-butyl acrylate ([M]/[I]=800) by initiator **1** (solid symbols) and initiator **5** (open symbols) catalyzed by CuBr/PMDETA in the presence of ethylene carbonate (11.4 mass %) at 100 °C*

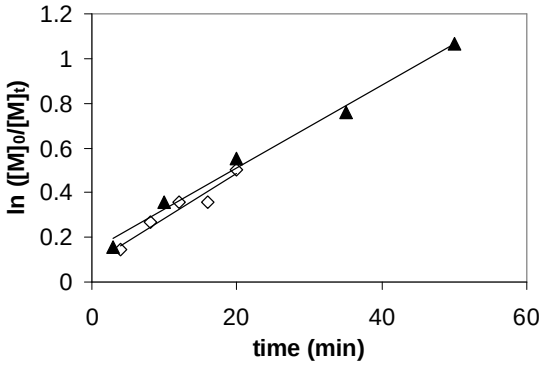

Figure 3 *Kinetic plot of monomer conversion as a function of reaction time for the polymerization of methyl methacrylate ([M]/[I] = 1600) by initiator **2** (open symbols) and initiator **6** (solid symbols) catalyzed by CuCl/HMTETA in diphenyl ether (50 volume %) at 90 °C*

In general, the polymerizations of tBA and MMA by the resorcinarene-based initiators showed controlled behavior, yielding star polymers with narrow molar mass distributions and molar masses close to theoretical ones.[I II, IV] The polymerizations were first order with respect to the monomer and had constant radical concentration. However, also some deviations from the controlled behavior were observed. A well-known side reaction in the preparation of branched polymers is bimolecular coupling. The coupling between the stars mostly depends on the reactivity of the monomer and thus, also on the reaction conditions.[51,52] The probability of the star-star coupling increases when the growing stars reach their critical overlap concentration c*.[52] Therefore, star-star coupling was observed for all polymerizations at high conversions (>30 %), leading to bimodal molar mass distributions and higher polydispersities. The threshold conversions for coupling were lower for the more reactive monomer (MMA) and more active ligands (PMDETA, HMTETA, Me_6TREN). In order to avoid star-star coupling, the conversions were kept low, particularly in the preparation of amphiphilic star polymers.

Other side reactions revealed by the kinetic studies and the evolution of molar masses include initial termination reactions, observed particularly for the polymerization of MMA, and catalyst poisoning during the polymerization of tBA, leading to slower polymerization or in some cases to complete termination.[II,IV] The catalyst may be

poisoned by traces of oxygen, by the elimination of HBr from the chain ends in polar medium (ethylene carbonate), or by the degradation of monomer via ester pyrolysis during the very slow polymerizations.[77,90] In addition, the spontaneous formation of deactivating species ($CuBr_2$ or $CuCl_2$) generated by a persistent radical effect may lead to termination reactions.[91]

3.2. Self-assembling of amphiphilic star block copolymers[III, V, VI]

3.2.1. Properties of the amphiphiles

The compositions of the amphiphilic star block copolymers are presented in Table 1. Four-arm and eight-arm stars were synthesized using initiators **2** and **6**, respectively, by the block copolymerization of methyl methacrylate and *tert*-butyl acrylate, followed by the hydrolysis of *tert*-butyl ester groups. The resulting (PMMA-*b*-PAA)$_n$ polymers were composed of hydrophobic poly(methyl methacrylate) core and hydrophilic poly(acrylic acid) shell (Scheme 10). Due to the polyelectrolyte nature of outer blocks, the solubility of the amphiphiles in water depended on the degree of ionization (α) of poly(acrylic acid) and thus, on pH. The polymers were not soluble in water below pH 4.5 (pH 4.7 for eight-arm stars) at low degree of ionization ($\alpha < 0.1$). The samples of four-arm (PMMA-*b*-PAA)$_4$ stars were prepared by the direct dissolution of the polymer in distilled water, whereas the dissolution of eight-arm (PMMA-*b*-PAA)$_8$ stars required a small addition of NaOH.

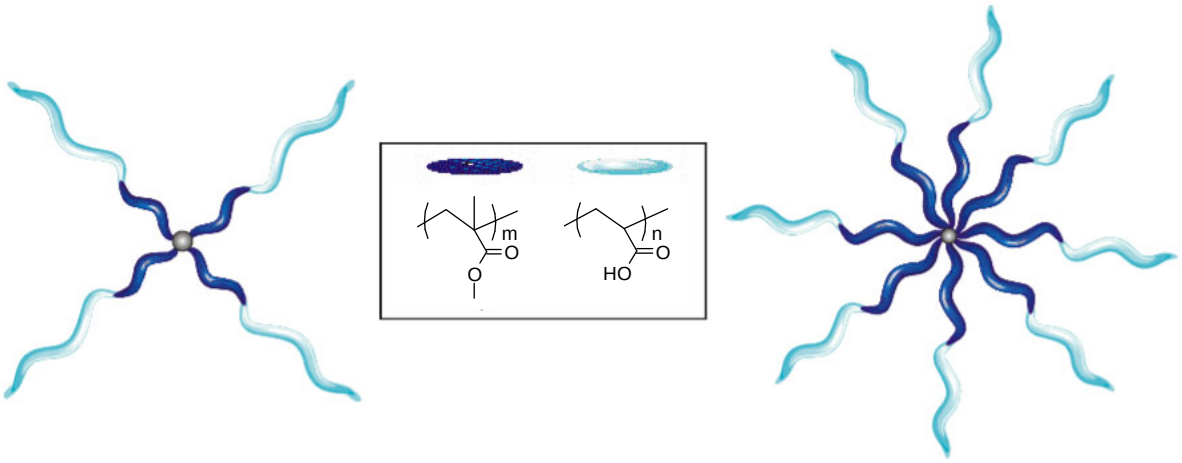

Scheme 10 *Schematic view of the structures of amphiphilic star block copolymers*

3.2.2. Four-arm stars in aqueous solutions[III, V]

3.2.2.1. Salt-free solutions[III]

In addition to "unimolecular micelles", amphiphilic star block copolymers form micelle-like aggregates in aqueous solutions in the pursuit to diminish the exposure of hydrophobic blocks to water, similar to their linear analogues.[92-96] Cryo-transmission electron micrographs (cryoTEM) of a salt-free aqueous solution of four-arm amphiphilic $(PMMA_{73}$-*b*-$PAA_{143})_4$ star (**16**) showed the coexistence of both spherical micelles and micellar species that could be described as elongated or clustered ones (Figure 4). Such solutions exhibited Newtonian flow below and shear thinning above the critical overlap concentration c* of the aggregates (1.7 g/L). The scaling behavior of strongly increasing relative viscosities η_{rel} ($\eta_{rel} = \eta_0/\eta_s$, where η_0 is the viscosity at the zero shear rate and η_s is the viscosity of the solvent) above c* was close to the theoretical scaling of linear polymers above c* ($\eta_{rel} \propto c^{2.5}$).[24,97] Since the concentration dependence of η_{rel} above c* reflects the softness of colloidal systems, it suggests along with the weak shear thinning behavior that the aggregated stars do not behave as hard spheres and they do not form an interconneted network at the studied concentration range.

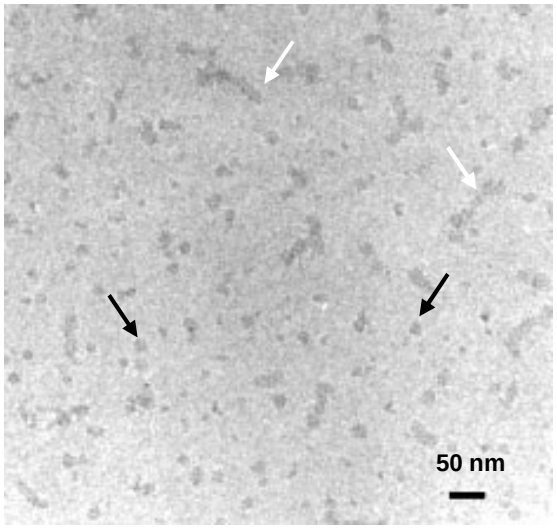

Figure 4 *Representative cryo-transmission electron micrograph of the ($PMMA_{73}$-b-$PAA_{143})_4$ star polymer (**16**) in 5 g/L salt-free aqueous solution (underfocus 6.8 μm). The black arrows point to spherical micelles and the white arrows to the elongated ones.*

The amphiphilic star showed striking time-dependent viscoelastic properties in a semidilute solution (15 g/L). The presheared sample (shear rate 1000 s^{-1}) behaved as viscous liquid with the loss modulus *G''* exceeding the storage modulus *G'* throughout the studied frequency range (Figure 5). The moduli scaled with frequency in a way typical for viscoelastic Maxwellian liquids: *G''* scaled with ω^2 and *G'* with ω. After the sample was

allowed to stand undisturbed in the measuring cylinder, the elastic modulus built up slowly and after 14 h, the sample reached a soft gel-like behavior with *G'>G''* over the entire studied frequency range. The fluid-like character reappeared upon shearing the gel.

The slow gelation may stem from the formation of a physical network by hydrophobic interactions or to the interpenetration of coronal layers, which has been described for the micellar systems of linear polyelectrolyte block copolymers.[98] Due to the repulsion between the poly(acrylic acid) chains in the absence of salt, the association between the micelles of amphiphilic stars can be easily broken after which the sample exhibits fluid-like character. Factors like high molar mass, low number of arms, large fraction of the hydrophobe and starlike architecture have been reported to favor the gelation of neutral block copolymers, such as the block copolymers of poly(L-lactide) and poly(ethylene oxide).[99]

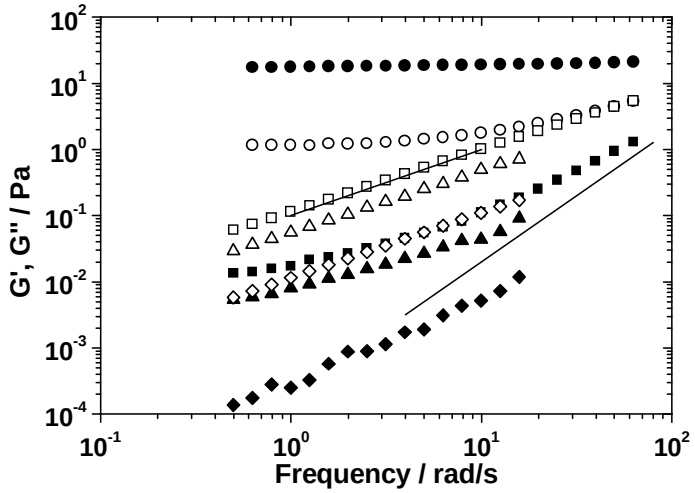

Figure 5 *Storage (G') and loss modulus(G'') vs. frequency of the amphiphilic ($PMMA_{73}$-b-$PAA_{143})_4$ star (**16**) at concentration of 15 g/L (■,□), 8.0 g/L (▲,Δ) and 3.9 g/L (♦,◊) in water directly after flow measurement and of 15 g/L (●○) after 14 h. Filled symbols are for G' and open symbols for G''. The straight lines show the theoretical scaling of the moduli as G' scales up ~ ω and G'' ~ ω^2.*

3.2.2.2. Saline solutions[III, V]

Adding salt (NaCl) to the aqueous solutions of four-arm amphiphilic ($PMMA_{73}$-*b*-$PAA_{143})_4$ star (**16**) with pH 4.5 reduced the viscosities close to that of the solvent and resulted in shear-induced precipitation due to decreased electrosteric stabilization of the aggregates. The saline solutions were opaque, indicating the presence of particles that are larger than in the absence of salt and that have sizes comparable to the wavelength of light.[III] When the pH of the saline solution was increased by adding NaOH, the solution became less cloudy and its normalized light scattering intensity decreased, indicating a decrease in the average molar mass or the density of the aggregates.[V] As the pH influenced the nature of the aggregates, the characteristics of the solutions with low and high pH values will be discussed below in separate sections.

Solutions at low pH (pH 4.5, 0.1 M NaCl)[III]

The distributions of relaxation times, τ, of correlation functions $G_1(t)$, over a range of polymer concentrations (0.031-8.53 g/L, presented in paper III) were determined by dynamic light scattering (DLS). Due to the generally ill-defined problem of fitting the correlation functions, Laplace inversion algorithm CONTIN is known to fail in some cases, such as broad size distributions.[100] Therefore, depending on the fitting parameters, the Laplace inversion gave either bimodal or broad monomodal distributions of relaxation times.

Other origins of bimodality could be intermolecular interactions (such as aggregation, too high polymer concentration, or the polyelectrolyte effect) or the coexistence of both rotational and translational diffusion processes typical for nonspherical species, such as rod-like micelles.[101,102] Only translational diffusion was observed through the linear dependence of the mean relaxation rates Γ on the squared amplitude of the scattering vector q^2 ($q=(4\pi n_0/\lambda_0)\sin(\theta/2)$, where n_0 is the refractive index of solvent, λ_0 is the wavelength in vacuum, and θ is the scattering angle).

The broad relaxation time distributions and large values of the mean hydrodynamic radius of the amphiphile, R_h(mean) = 111 nm (at 0.625 g/L), suggest the intermolecular association of the stars. The values of R_h(mean) are larger than the theoretical maximum radius of a single star given by the contour length of an arm, R_{theor} = 54 nm, or the hydrodynamic radius of the hydrophobic ($PMMA_{73}$-*b*-$ptBA_{143})_4$ precursor in good solvent (THF), R_h = 7.9 nm. Static light scattering (SLS) of the aqueous solutions gave the weight-average molar mass $M_w = 28.6 \times 10^6$ g/mol, corresponding to an aggregation number N_{agg} ~300.

The aggregates were rather stable towards dilution, long storage (6 weeks at +5 °C) or gradual heating to 50° C (within 4 h). The shape of the autocorrelation functions $G_2(t)$ at 30° measuring angle did not change considerably upon decreasing polymer concentration from 5.0 g/L to 0.25 g/L though the mean relaxation time shifted towards lower values (Figure 6). Also the normalized second cumulant $(\mu_2/\Gamma^2)q^2$, representing the polydispersity of the decay rate distribution at 0° scattering angle, was nearly constant. The stability of the aggregates arises from the high glass transition temperature T_g of PMMA block hindering the chain exchange between the micelles[103] and from the electrosteric stabilization by the hydrophilic blocks despite the screening of charges by salt.[103,104] Higher salt concentrations (0.15 M) led to precipitation.

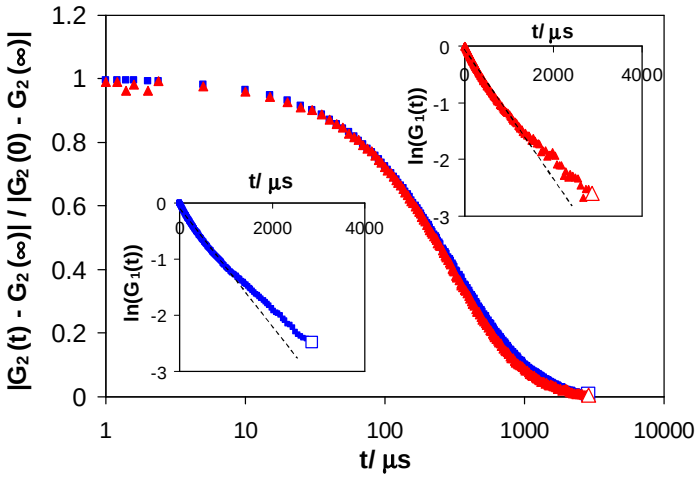

Figure 6 *Examples of normalized autocorrelation functions of the intensity of scattered light, $G_2(t)$, measured at 20 °C and 30° scattering angle. Solid blue square (■) corresponds to polymer concentration 5 g/L and red triangle (▲) to 0.25 g/L, both at aqueous 0.1 M NaCl solution. The insets show corresponding correlation functions of electric field, $G_1(t)$, where dashed lines have been added as guide for eye and correspond to a single exponential decay. Enlarged open symbols show the data points corresponding to the same delay time of the functions.*

The angular dependence of the average values of the diffusion coefficient $D_\theta = \Gamma/q^2$ at the whole range of polymer concentrations indicated that the aggregates were either polydisperse or their shape was not spherical. The radius of gyration (R_g) of the amphiphile was calculated for two concentrations, 5 g/L and 1.25 g/L, from the linear region of particle scattering function, $P(q) = R_\theta/R_{\theta=0}$, which gave the values of R_g=127.9 nm and 162.5 nm, respectively. Figure 7 shows Kratky representation $(qR_g)^2P(q)$ versus qR_g for solutions with the same polymer concentrations. At the low values of qR_g, the particles resemble a random coil as they are seen in the scattering experiment comprising of a large number of Kuhn segments, and therefore, at this range of qR_g all the theoretical particle scattering functions shown in Figure 7 coincide.[105,106]

At the high values of qR_g ($qR_g > 2$), shorter sections of the particles are probed and the structure of the particles can be revealed by the Kratky plot, in which the asymptotic part is strongly amplified making the differences in structures distinguishable. Thus, for starlike polymers with a low number of arms a model of a random coil may still be valid, whereas increasing the number of arms leads to the Debye-Bueche behavior typically describing branched structures.[107,108] The experimental data obtained from the 5 g/L solutions of the amphiphilic stars in the $qR_g > 2$ region coincide well with the theoretical predictions representing either polydisperse rods[109] or wormlike chains.[110,111] The difference between the curves of two polymer concentrations may arise from the polydispersity of the structures formed in the 1.25 g/L solution.

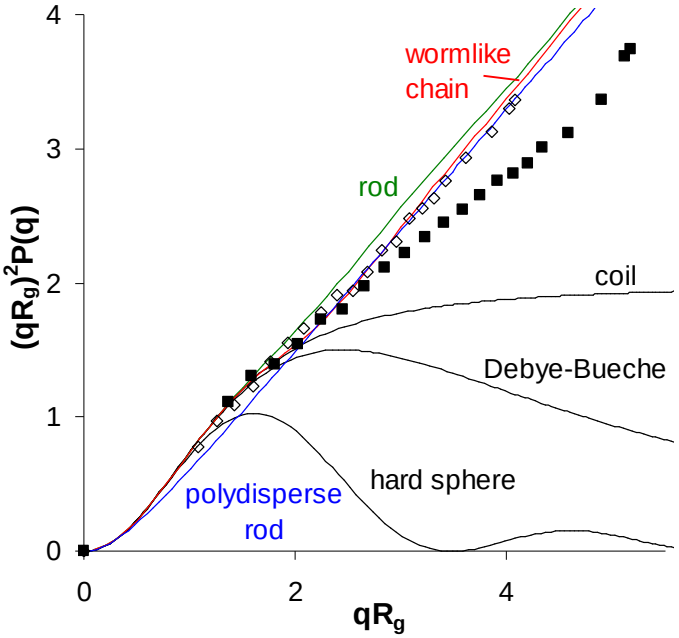

Figure 7 *Kratky representation $(qR_g)^2P(q)$ versus qR_g of the experimental particle scattering functions, $P(q) = R_\theta/R_{\theta=0}$, for 5 g/L (open symbols) and 1.25 g/L (solid symbols) solutions of the four-arm amphiphilic star. Theoretical curves for model macromolecular structures have been added for comparison as solid lines.*

CryoTEM was employed to visualize the structures formed in the same solutions as above and thus, to verify the conclusions from the light scattering data. The micrographs (Figure 8) of a 5 g/L solution of the amphiphile revealed the coexistence of two major classes of particles: small spherical micelle-like aggregates (the diameter of the dark core, D_{core}= 19 $\pm$ 3 nm) and larger curved worm-like aggregates of varying lengths (195 $\pm$ 25 nm), both with rough edges and visible radiating arms from the dark core. Comparison with the Kratky representation (Figure 7) shows that the scattering is primarily determined by the large worm-like species and hence, the scattering from smaller spherical species is engulfed.

The results above indicate that the addition of salt triggers the formation of the worm-like micelles of amphiphilic star block copolymers. Micellar morphologies depend on the extension of the hydrophobic blocks in the micellar core, the surface tension between the core and the solvent, and the repulsion between the hydrophilic blocks in the corona.[22,112] When the hydrophilic block is ionic, like poly(acrylic acid), the balance between these factors can be altered by adding salt, which decreases the electrostatic repulsion in the corona, favoring the aggregation of amphiphiles.[103,113,114]

Israelachvili and coworkers[3] have developed a theoretical approach predicting micellar morphologies using geometrical considerations. In this approach, the major forces governing the self-assembling behavior of low-molar-mass surfactants, but also of amphiphilic block copolymers, are the attraction between the hydrophobic moieties and

the repulsion between the hydrophilic groups due to electrostatic or steric interactions. If the attractive forces predominate, the interfacial area a_0 per molecule will decrease, and if the repulsive forces predominate, a_0 will increase. The packing parameter p of micelles, also known as the shape factor, depends on the interfacial area a_0, the volume v occupied by the hydrophobic chains and their maximum length l_c ($p = v/(a_0 l_c)$). Spherical micelles have a high interfacial curvature and low values of p ($p < 1/3$) while cylindrical micelles have a lower curvature and higher values of p ($p = 1/3 – 1/2$). The screening of charges by added salt would result in a lower interfacial area a_0 per molecule and thus, a higher packing parameter p. This will lead to a sphere-to-cylinder transition of micelles, if the packing parameter exceeds the limiting value 1/3.[3]

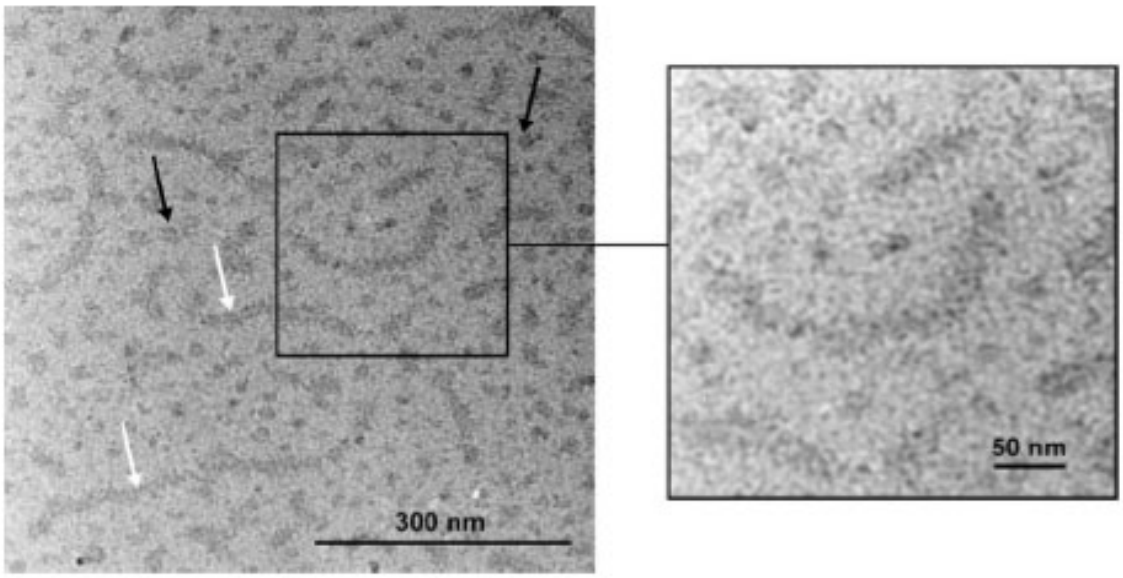

Figure 8 *Representative cryo-transmission electron micrographs of ($PMMA_{73}$-b-PAA_{143})$_4$ star polymer (**16**) in 5 g/L aqueous 0.1 M NaCl solution (underfocus 8.4 μm). The black arrows point to spherical micelles and the white arrows to the wormlike ones. Inset shows an enlargement of micelles displaying radiating arms.*

Increasing the aggregate size is thermodynamically favorable in order to reduce the interfacial area between the solvent and the hydrophobic core. However, further aggregation would lead to an increase in the radius of the core and stretching of the chains. Hence, according to Zhang and Eisenberg[112], an additional degree of freedom could be attained without significant changes in conformation by changing the micellar morphology from spherical to cylindrical, which will result in a lower interfacial curvature. The formation of wormlike micelles and their coexistence with the spherical ones has been observed earlier for linear amphiphiles with varying compositions and block ratios, both experimentally and theoretically[5,115,116], as well as for amphiphilic heteroarm star copolymers in which the arms rearrange to separate hydrophobic and hydrophilic domains.[117]

Solutions at high pH (pH 12.7, 80 mM NaCl)[V]

In another series of experiments, the starting pH of the solution was slightly higher, pH = 5.0. Although the increase in pH of 5 g/L aqueous solution of ($PMMA_{73}$-*b*-PAA_{143})$_4$ star from pH 5.0 to pH 12.7 led to a decrease in the intensity of scattered light, the relaxation time distributions and the autocorrelation functions of scattered light obtained by DLS were identical at 90° measuring angle. A small difference was observed in the shape of the autocorrelation functions at 35° measuring angle (Figure 9), indicating that the solution of the amphiphile consists of larger aggregates at pH 5.0 than at pH 12.7, thus explaining the higher turbidity at low pH. Since the large species dominate the scattering behavior, this difference was not observed at 90° angle. At high pH, the light scattering behavior did not depend on the way of sample preparation, that is, whether the polymer was dissolved at high or low pH prior to the addition of salt. The results by DLS and cryoTEM also indicated that the formation of worm-like micelles observed at low pH was reversible.

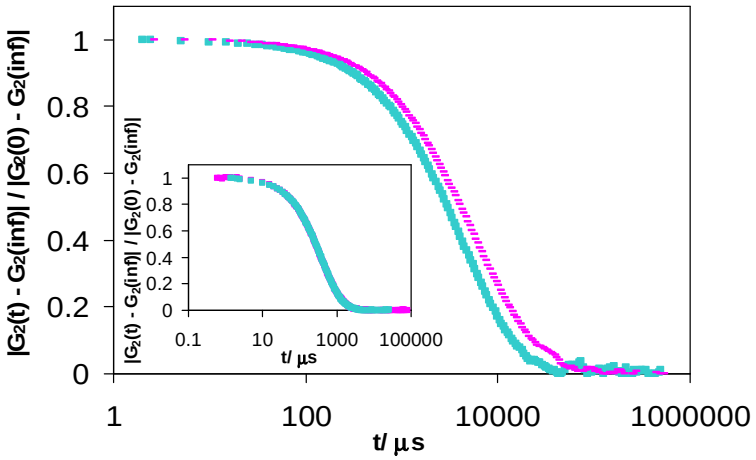

Figure 9 *Normalized autocorrelation functions of scattered light intensity, $G_2(t)$, measured at 35° scattering angle for aqueous 5 g/L solution of ($PMMA_{73}$-b-PAA_{143})$_4$ (**16**). Pink symbol (■) corresponds to pH 5.0 and turquoise one (■) to pH 12.7. The inset shows overlapping autocorrelation functions of the same samples at 90° scattering angle.*

According to the correlation functions of electric field $G_1(t)$ and the relaxation time distributions, the samples were highly polydisperse, which along with the presence of large scatterers makes it difficult to estimate the difference in the densities of the species. Therefore, cryoTEM was utilized to obtain further information on the aggregates. The micrographs of the amphiphile at pH 12.7 (some examples in Figures 10-11) show that the sample mainly consists of spherical micelles (D_{core} = 25 $\pm$ 6 nm), but there are also some larger elongated aggregates having loose "pearl-necklace" structure (Figure 11). In accordance with the light scattering results, the fraction of worm-like species was lower than at low pH. While the worm-like micelles were intact at pH 4.5 (Figure 8), those with "pearl-necklace" structure pH 12.7 seem to be composed of smaller spherical species, which could arise from the disintegration of larger aggregates either due to the increased repulsion between the ionized poly(acrylic acid) blocks or swelling of the polyelectrolyte

corona, as suggested by the decrease in the light scattering intensity upon increasing pH. Considering the model by Israelachvili and coworkers[3] presented above, higher repulsion within the corona would result in a higher interfacial area a_0 per molecule, leading to a lower packing parameter p associated with the higher interfacial curvature. This change in the interfacial area may induce a morphological transition. Similar observations on the pH-induced transitions between micellar morphologies have been reported for linear amphiphilic block copolymers with poly(acrylic acid) blocks.[115,118]

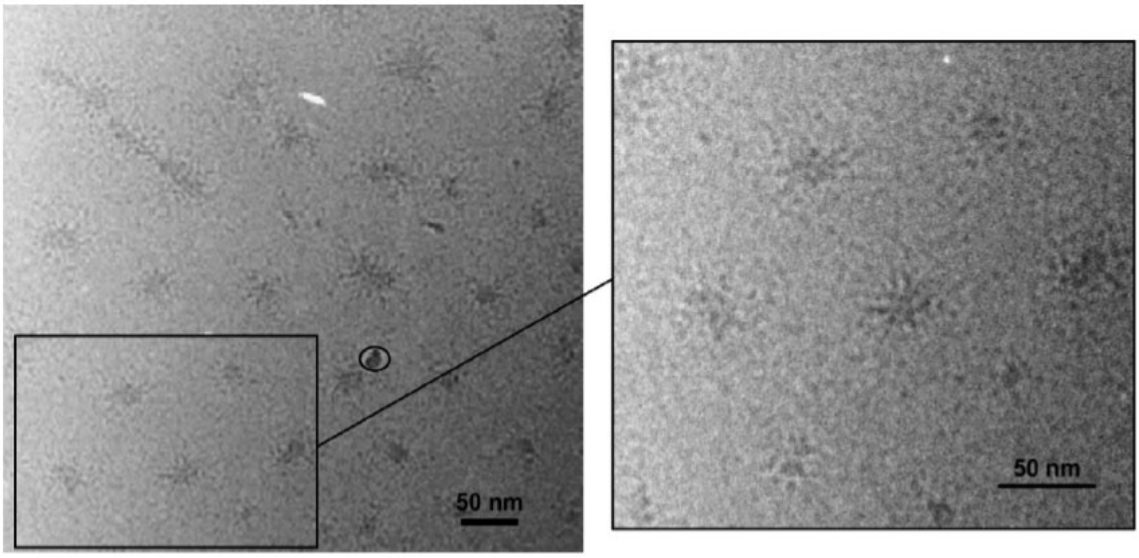

Figure 10 *A cryo-transmission electron micrograph of ($PMMA_{73}$-b-PAA_{143})$_4$ (**16**) star polymer in 5 g/L aqueous NaCl solution with pH 12.7 and ionic strength 80 mM (underfocus 7 μm). The defect in the image from ice has been circled.*

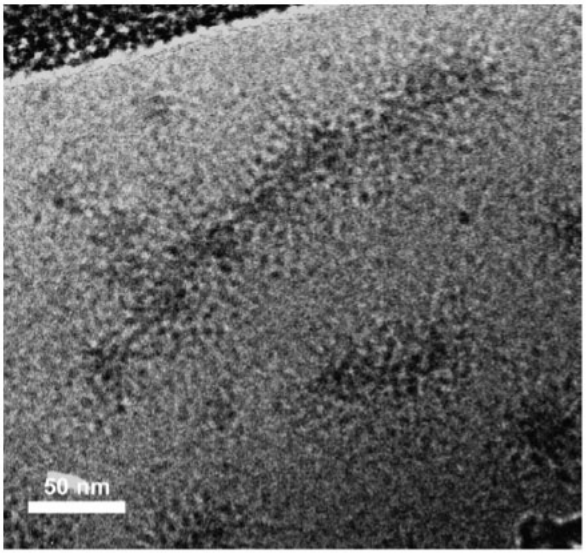

Figure 11 *An enlargement of the cryo-transmission electron micrograph of ($PMMA_{73}$-b-PAA_{143})$_4$ (**16**) star polymer in 5 g/L aqueous NaCl solution with pH 12.7 and ionic strength 80 mM (underfocus 7 μm). The image shows the 'pearl-necklace' structure of a disintegrated worm-like micelle.*

The disintegration of the worm-like aggregates at high pH is in agreement with the results of coarse-grained computer simulations using the same architecture and the same length ratio of hydrophobic and hydrophilic blocks (Figure 12). Detailed descriptions of the model and the simulations are presented in paper V. When the degree of ionization α of the polyelectrolyte outer block approached zero (pH < 5), the model amphiphilic stars aggregated into worm-like micelles. At a high degree of ionization (α = 1, pH = 12), mainly spherical micelles with highly stretched coronas were observed. It was suggested that the stretching of the corona at high pH stems rather from a high osmotic pressure than from the repulsion between the charged units, as most of the counterions are trapped to the corona of the micelles. High osmotic pressure will lead to the swelling of the corona.[V]

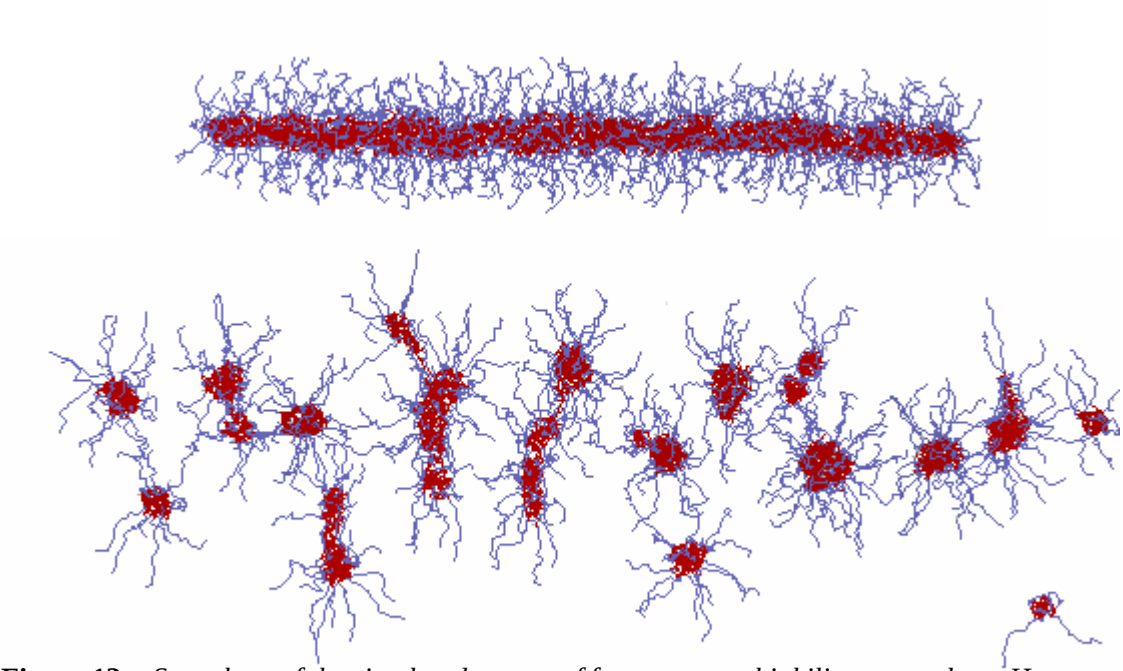

Figure 12 *Snapshots of the simulated system of four-arm amphiphilic stars at low pH (uncharged) above and at high pH (charged) below; shown without counterions.*

3.2.3. Eight-arm stars in aqueous solutions[VI]

As the number of arms was expected to influence the interfacial curvature of starlike amphiphiles and thus, their self-assembling characteristics, the properties of two eight-arm amphiphilic star block copolymers, $(PMMA_{77}\text{-}b\text{-}PAA_{86})_8$ (**19**) and $(PMMA_{65}\text{-}b\text{-}PAA_{108})_8$ (**22**), were investigated in aqueous solutions. The block ratios (PMMA:PAA) were 1:1.1 and 1:1.7, respectively. The critical aggregation concentrations (cac) of the amphiphiles in salt-free solution (degree of ionization α = 0.25) were determined by the steady-state fluorescence spectroscopy of 4HP (**23**, Scheme 11) as well as from the onset of increasing light scattering intensities. The values of cac were expectedly lower for the amphiphile **19** with a longer hydrophobic block and a higher fraction of the hydrophobe, being $(0.35 \pm 0.04) \times 10^{-3}$ g/L when determined by fluorescence spectroscopy and $(0.80 \pm 0.21) \times 10^{-3}$

g/L by LS.[†] The corresponding values for the amphiphile **22** were (0.90 ± 0.05) × 10^{-3} g/L and (1.80 ± 0.44) × 10^{-3} g/L, respectively. The difference between the values given by these two methods may arise from the differences in the principles of the methods: while light scattering is a noninvasive method that requires no external probe, fluorescence spectroscopy utilizes a hydrophobic probe that may perturb the hydrophobic interactions despite its low concentration.

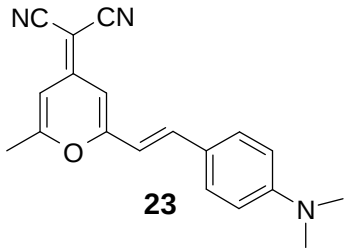

23

Scheme 11 *Structure of 4-(dicyanomethylene)-2-methyl-6-(*p*-dimethylaminostyryl)-4*H*-pyran (4HP, also called DCM).*

The characteristics of the amphiphiles were investigated above their critical aggregation concentration at a constant polymer concentration (5.0 g/L), but varying the pH and ionic strength of the solutions. Dynamic light scattering gave bimodal relaxation time distributions in which both relaxation processes originate from translational diffusion. The diffusion coefficients $\Gamma/q^2 = D_\theta$, obtained from the mean relaxation rates Γ plotted as the function of squared amplitude of the scattering vector q^2, were used to calculate the hydrodynamic radii (R_h) of the relaxation processes from the Stokes-Einstein relation:

(2) $$D_\theta = \frac{kT}{6\pi\eta R_h},$$

in which η is the viscosity of the medium and R_h is the hydrodynamic radius. The average values of R_h in aqueous NaCl solutions (0.1– 0.4 M) were 19 nm and 20 nm for the fast mode for amphiphiles **19** and **22**, respectively. Since the angular dependence of the diffusion coefficients of the fast mode was minor and the hydrodynamic radii corresponded to the ones obtained from cryoTEM images (Figure 13), 17 nm and 18 nm, we may conclude that the fast mode corresponds to spherical species.

The cryoTEM micrographs revealed the presence of a small fraction of large clusters in saline solutions, these most probably being the origin of the slow diffusion mode. The sizes of such clusters were within the error of the hydrodynamic radii determined by DLS, 183 nm for polymer **19** and 247 nm for **22**. The presence of large clusters or aggregates is

[†] *The cac determined by LS for a sample of polymer **19** with 95% degree of hydrolysis gave cac (0.85 ± 0.26) × 10^{-3} g/L. This value is within the error of the value above for the sample with lower degree of hydrolysis (polymer **19** with 89% of the tert-butyl ester groups). Therefore, it may be concluded that the remaining* tert*-butyl ester groups had only minor effect on the cac.*

often characteristic of block copolymer samples prepared by the direct dissolution method, as the dissolution of the polymer occurs by the slow fragmentation of powder into smaller parts.[103] However, some large aggregates of irregular shapes were observed in the computer simulations of the amphiphiles in saline solutions and hence, they could also be formed by further aggregation of stars upon screening of the charges of the polyelectrolyte blocks.

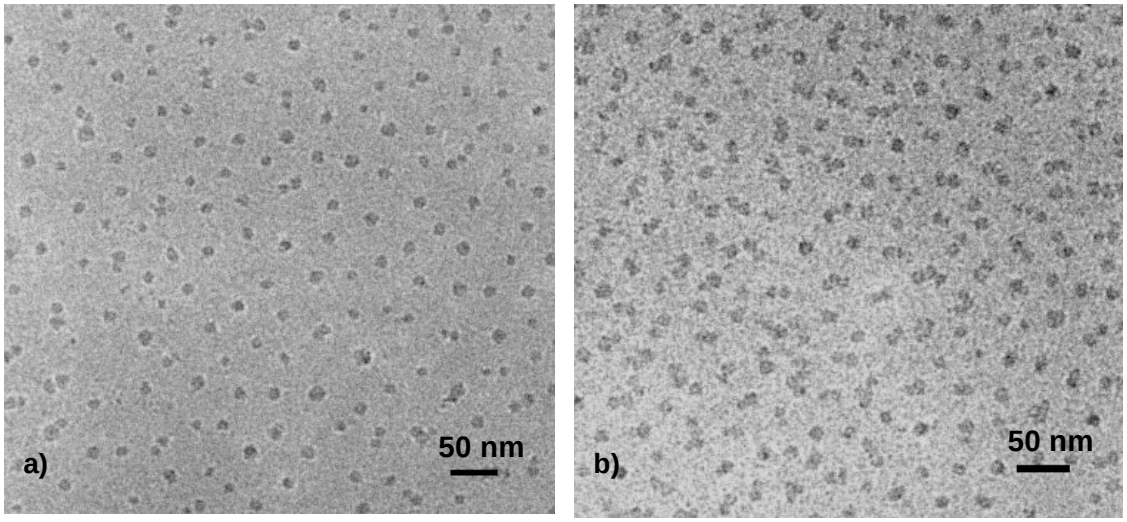

Figure 13 *Representative cryoTEM micrographs of aqueous 5 g/L solutions of ($PMMA_{65}$-b-$PAA_{108})_8$ (**22**) at pH 4.9 a) in the absence of salt (underfocus 7.6 µm) and b) in 0.1 M NaCl (underfocus 7.7 µm).*

The maximum dimensions of single stars were estimated from the contour lengths of the hydrophobic and hydrophilic blocks the arms, giving the maximum radii of the core and the shell, R_c(max, theor) and R_s(max, theor) in Table 2, respectively. The minimum radii of the cores of single stars were 1.10 nm (**19**) and 1.07 nm (**22**), estimated from the equation:

(3) $$\frac{4}{3}\pi R_c^{\,3} = N_{agg} N_{MMA} \upsilon_0 ,$$

in which N_{MMA} is the number of MMA units in one block and υ_0 is the molar volume of one MMA unit.[119] These values were considerably lower than those obtained from cryoTEM micrographs (R_c in Table 2), and because the PMMA cores are in a collapsed state in aqueous medium, we may assume that the spherical species observed above the cac of the amphiphiles are multimolecular micelles.

As the presence of large particles impedes determining the molar masses of smaller species by static light scattering, equation (3) was used in estimating the aggregation numbers N_{agg} for spherical micelles from R_c. The average aggregation numbers were 13 (for **19**) and 11 (for **22**), which are in a reasonable agreement with the theoretical aggregation numbers N_{agg}(theor) (19 and 11, respectively) given by the model by Förster

and coworkers.[119] According to this model, the aggregation number of amphiphilic block copolymers is dependent on the lengths of both hydrophobic and hydrophilic blocks:

(4) $$N_{agg} = Z_0 N_A^{\ 2} N_B^{\ -0.8},$$

in which N_A is the length of hydrophobic block and N_B is the length of hydrophilic block. Z_0 is the local packing parameter at the core/corona interface, being 0.9 for linear block copolymers of PMMA and PAA.[120] The results suggest that the same model, which has earlier been used to predict the aggregation behavior of starlike block copolymers with three arms[92], would also apply to stars with higher number of arms.

While the addition of salt screened the charges and thus decreased the radius of the polyelectrolyte shell of the micelles, the increase in pH of the solutions resulted in the stretching of the poly(acrylic acid) blocks up to ~90 % of their contour length (Table 2). This was also reflected by lower values of R_g/R_h at high pH. The values of R_g/R_h were lower than the hard-sphere limit 0.78 due to the soft corona surrounding the hard core of the micelles[121,122], being closer to this limit for the amphiphile **19** with shorter hydrophilic blocks. Coarse-grained computer simulations of eight-arm stars with the length ratio of hydrophobic and hydrophilic blocks similar to amphiphile **19** (Figure 14) showed that adding salt resulted in a lower degree of stretching of both blocks. The screening of charges increased the aggregation number of stars, which was observed both at low and high pH. Nevertheless, eight-arm stars exhibited only spherical micelles and larger irregular aggregates, while according to the simulations, four-arm stars with the same composition formed cylindrical micelles in the presence of salt.[VI] The results suggest that the aggregation behavior of stars is strongly dependent on the number of arms. Increasing the number of arms increases the degree of stretching of hydrophobic blocks and results in higher repulsion between the hydrophilic blocks. Such aggregates with a high interfacial curvature prefer spherical morphology.[3,58] Therefore, the high number of arms prevents the formation of large aggregates as well as the transition between the micellar morphologies.

Table 2. *Properties of the spherical micelles from the cryoTEM and light scattering results.*

Entry	Solution	R_c(max, theor)[a]/ nm	R_s(max, theor)[b]/ nm	R_c/ nm	R_s/ nm	R_s/R_s(max)[c]	R_s/R_c	N_{agg}[d]	R_{tot}/ nm	R_h(DLS)[e]/nm	R_g/R_h[e]
	no salt, pH 4.9	19.2	21.5	6.5 ± 0.8	12.1 ± 4.2	0.56	1.9	13 ± 5	18.6 ± 5.0		
19	0.1 M NaCl pH 4.9			6.4 ± 0.7	10.5 ± 2.6	0.49	1.6	13 ± 4	16.9 ± 3.3	19.4 ± 1.3	0.73
	0.1 M NaCl pH 12.5			6.2 ± 0.7	20.0 ± 2.4	0.93	3.2	12 ± 4	26.2 ± 3.1	19.4 ± 0.3	0.69
	no salt, pH 4.9	16.1	27.1	5.7 ± 0.8	16.3 ± 3.0	0.60	2.9	10 ± 6	22.0 ± 3.8		
22	0.1 M NaCl pH 4.9			5.7 ± 0.6	11.7 ± 2.2	0.43	2.0	12 ± 5	17.6 ± 2.8	20.7 ± 1.3	0.63
	0.1 M NaCl pH 11.9			5.8 ± 0.6	22.9 ± 2.1	0.85	3.9	11 ± 5	28.7 ± 2.7	19.9 ± 0.9	0.54

a) Theoretical maximum radius of the core given by the contour length of the hydrophobic PMMA block in a single arm, calculated from the repeating units.
b) Theoretical maximum radius of the shell given by the contour length of the hydrophilic PAA block in a single arm, calculated from the repeating units.
c) R_s/R_s(max, theor), describes the stretching of PAA blocks.
d) Calculated from the equation: $(4\pi R_c^3)/3 = N_{agg} \times N_{MMA} \times \nu_0$, in which N_{MMA} is the amount of MMA units in one block, N_{agg} is the number of blocks in the micellar core, and ν_0 is the molar volume of MMA unit.
e) Calculated as average values from the measurements at pH 5.1 and pH 9.2, respectively.

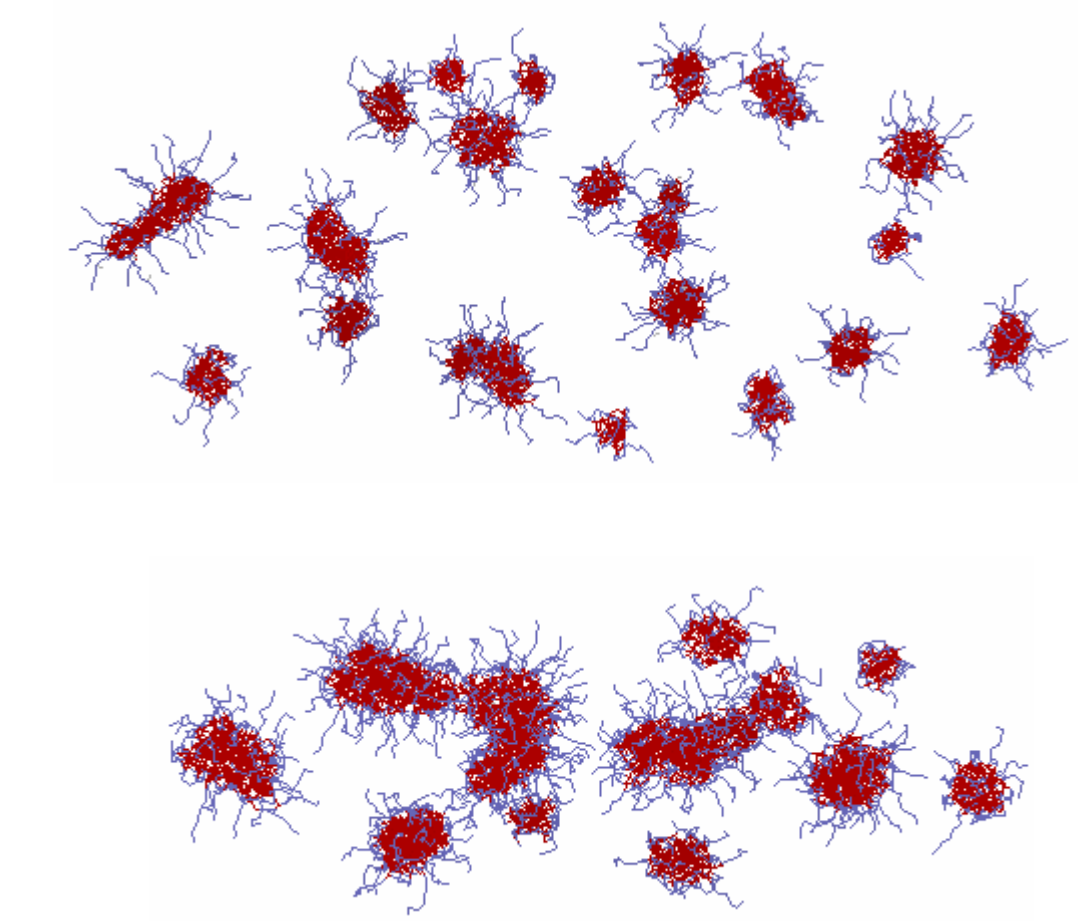

Figure 14 *Snapshots of the simulated system of eight-arm amphiphilic stars in saltfree solution (above) and in the presence of salt (below); shown without counterions.*

4. Conclusions

The main objective of the current research has been to investigate the self-assembling behavior of amphiphilic star diblock copolymers in aqueous solutions. As the preparation of well-defined polymer architectures is essential in order to achieve understanding about the structure-property relationship, a major part of the work has focused on the synthesis of star polymers. The current work also considers various aspects related to the number of arms (functionality *f*) in stars, from the synthesis of multifunctional initiators to the self-assembling characteristics of star block copolymers with different *f*. In parallel with the experiments, molecular modeling or computer simulations were successfully employed both in the conformational studies of the initiators as well as in exploring the amphiphilic stars.

The preparation of multifunctional initiators for atom transfer radical polymerization (ATRP) by derivatizing macrocyclic compounds, resorcinarenes, altered the conformation of the macrocyclic ring thus bringing a part of the substituents in proximity to each other. This may result in the intermolecular coupling of radicals. Therefore, rigid initiators without a spacer between the initiating sites and the macrocyclic ring gave polymers with a lower number of arms than the flexible ones equipped with a spacer. The steric hindrance of the initiating sites decreased also the polymerization rate of a bulky monomer, *tert*-butyl acrylate. Reducing the steric hindrance of the catalyst had no effect on the functionalities of stars, but it influenced the controllability of the polymerization. The rigid and the flexible initiators were used to the syntheses of amphiphilic star block copolymers of poly(methyl methacrylate) and poly(acrylic acid) with four and eight arms, respectively. Poly(acrylic acid) blocks were obtained by the selective cleavage of *tert*-butyl ester groups of poly(*tert*-butyl acrylate).

Amphiphilic star block copolymers with a hydrophobic core and hydrophilic corona have often been treated as representatives of unimolecular micelles in dilute solutions. In addition, as shown in the current study they are capable of forming multimolecular assemblies in solution. Such self-assemblies can be spherical or wormlike, depending on the ionic strength and pH of the solution, and more importantly, on the number of arms in the stars. Stars with a low number of arms (4) associated in the similar way as linear block copolymers, forming both spherical and wormlike aggregates, the latter upon the screening of charges by the addition of salt. The wormlike species disintegrated at high pH into spherical micelles due to a higher degree of ionization of the polyelectrolyte blocks. In addition, the high osmotic pressure by trapped counterions led to the swelling of the corona. In salt-free solutions, the four-arm stars exhibited time-dependent gelation due to the formation of a physical network by hydrophobic interactions or to the interpenetration of coronal layers of the micelle-like aggregates. Stars with a high number of arms (8) formed only spherical micelles in spite of added salt, because of the higher stretching of the core-forming blocks as well as the higher repulsion between the polyelectrolyte blocks in the corona. The experimental findings were supported by the computer simulations.

The cylindrical self-assemblies of amphiphilic block copolymers may be utilized as drug delivery vehicles resembling natural filamentous phages with longer circulation times *in vivo* than spherical carriers.[123] Other possible applications could include unimolecular and self-assembled nanoreactors.[124] The self-assemblies of four-arm amphiphilic star diblock copolymers mimic those of globular cytoskeletal proteins, such as tubulin or actin, which contain acidic groups to provide polyelectrolyte nature.[125] In laboratory conditions, the self-assembling of these proteins into tubules or filaments can be triggered by the addition of salt and for instance, a globular G-actin forms filamentous F-actin in the presence of both monovalent and divalent salts.[126] Therefore, the investigated polymers have a profound importance not only due to their potential applications but also because they help in understanding and mimicking the complex processes occurring in nature.

5. Appendix

IUPAC names and CAS numbers of the resorcinarene derivatives, entries corresponding to those presented in Section 2.

1 2,8,14,20-tetraethylpentacyclo[19.3.1.$1^{3,7}$.$1^{9,13}$.$1^{15,19}$]octacosa-1(25),3(28),4,6,9(27),10,12,15(26),16,18,21,23-dodecaene-4,6,10,12,16,18,22,24-octayl octakis (2-bromopropanoate) (*CAS 778613-19-7*)

2 2,8,14,20-tetraethylpentacyclo[19.3.1.$1^{3,7}$.$1^{9,13}$.$1^{15,19}$]octacosa-1(25),3(28),4,6,9(27),10,12,15(26),16,18,21,23-dodecaene-4,6,10,12,16,18,22,24-octayl octakis (2-bromo-2-methylpropanoate) (*CAS 778613-20-0*)

3 octaethyl 2,2',2'',2''',2'''',2''''',2'''''',2''''''-[[2,8,14,20-tetramethylpentacyclo[19.3.1.$1^{3,7}$.$1^{9,13}$.$1^{15,19}$]octacosa-1(25),3(28),4,6,9(27),10,12,15(26),16,18,21,23-dodecaene-4,6,10,12,16,18,22,24-octayl]octakis(oxy)]octaacetate (*CAS 171799-35-2*)

4 2,2',2'',2''',2'''',2''''',2''''''-[[2,8,14,20-tetramethylpentacyclo[19.3.1.$1^{3,7}$.$1^{9,13}$.$1^{15,19}$]octacosa-1(25),3(28),4,6,9(27),10,12,15(26),16,18,21,23-dodecaene-4,6,10,12,16,18,22,24-octayl]octakis(oxy)]octaethanol (*CAS 65378-51-0*)

5 [2,8,14,20-tetramethylpentacyclo[19.3.1.$1^{3,7}$.$1^{9,13}$.$1^{15,19}$]octacosa-1(25),3(28),4,6,9(27),10,12,15(26),16,18,21,23-dodecaene-4,6,10,12,16,18,22,24-octayl] octakis(oxyethane-2,1-diyl) octakis(2-bromopropanoate) (*CAS 946502-71-2*)

6 [2,8,14,20-tetramethylpentacyclo[19.3.1.$1^{3,7}$.$1^{9,13}$.$1^{15,19}$]octacosa-1(25),3(28),4,6,9(27),10,12,15(26),16,18,21,23-dodecaene-4,6,10,12,16,18,22,24-octayl] octakis(oxyethane-2,1-diyl) octakis(2-bromo-2-methylpropanoate) (*CAS 946502-72-3*)

The IUPAC names were obtained using the ACD/I-Lab Web service (ACD/IUPAC Name 8.05).CAS numbers were obtained from CAS REGISTRY^{SM} database.

6. References

1. Rodríguez-Hernández, J.; Chécot, F.; Gnanou, Y.; Lecommandoux, S. *Prog. Polym. Sci.* **2005**, *30*, 691-724.

2. Mecke, A.; Dittrich, C.; Meier, W. *Soft Matter* **2006**, *2*, 751-759.

3. Israelachvili, J.N. Intermolecular and Surface Forces, 2nd edition. London: Academic Press, 1992, pp. 385-421.

4. Won, Y.-Y.; Bates, F. S. in: Zana, R.; Kaler, E.W., editors. Giant Micelles: Properties and Applications. Boca Raton, FL: CRC Press/Taylor & Francis, 2007, pp. 417-451.

5. Choucair, A.; Eisenberg, A. *Eur. Phys. J. E* **2003**, *10*, 37-44.

6. Hamley, I.W. *Angew. Chem. Int. Ed.* **2003**, *42*, 1692-1712.

7. Lazzari, M.; López-Quintela, M.A. *Adv. Mat.* **2003**, *15*, 1583-1594.

8. Duncan, R. *Nature Rev. Drug Discov.* **2003**, *2*, 347-360.

9. Discher, D.E.; Eisenberg, A. *Science* **2002**, *297*, 967-973.

10. Ternat, C.; Kreutzer, G.; Plummer, C.J.G.; Nguyen, T.Q.; Hermann, A.; Ouali, L.; Sommer, H.; Fieber, W.; Velazco, M.I.; Klok, H.-A.; Månson, J-A.E. *Macromol. Chem. Phys.* **2007**, *208*, 131-145.

11. Riess, G. *Prog. Polym. Sci.* **2003**, *28*, 1107-1170.

12. Nikova, A.T.; Gordon, V.D.; Cristobal, G.; Talingting, M.R.; Bell, D.C.; Evans, C.; Joanicot, M.; Zasadzinski, J.A.; Weitz, D.A. *Macromolecules* **2004**, *37*, 2215-2218.

13. Garnier, S.; Laschewsky, A. *Langmuir* **2006**, *22*, 4044-4053.

14. Save, M.; Manguian, M.; Chassenieux, C.; Charleux, B. *Macromolecules* **2005**, *38*, 280-289.

15. Tauer, K.; Zimmermann, A.; Schlaad, H. *Macromol. Chem. Phys.* **2002**, *203*, 319-327.

16. Riess, G.; Labbe, C. *Macromol. Rapid Commun.* **2004**, *25*, 401-435.

17. Nichifor, M.; Zhu, X.X. *Colloid Polym. Sci.* **2003**, *281*, 1034-1039.

18. Gitsov, I.; Fréchet, J.M.J. *J. Am. Chem. Soc.* **1996**, *118*, 3785-3786.

19. Yoo, M.; Heise, A.; Hedrick, J.L.; Miller, R.D.; Frank, C.W. *Macromolecules* **2003**, *36*, 268-271.

20. Semenov, A.N.; Vlassopoulos, D.; Fytas, G.; Vlachos, G.; Fleischer, G.; Roovers, J. *Langmuir* **1999**, *15*, 358-368.

21. Grest, G.S.; Fetters, L.J.; Huang, J.S.; Richter, D. *Adv. Chem. Phys.* **1996**, *XCIV*, 67-163.

22. Halperin, A.; Tirrell, M.; Lodge, T.P. *Adv. Polym. Sci.* **1992**, *100*, 31-71.

23. Daoud, M.; Cotton, J.P. *J. Phys. (Paris)* **1982**, *43*, 531-538.

24. Vlassopoulos, D.; Fytas, G.; Pispas, S.; Hadjichristidis, N. *Physica B* **2001**, *296*, 184-189.

25. Huber, K.; Bantle, S.; Burchard, W.; Fetters, L.J. *Macromolecules* **1986**, *19*, 1404-1411.

26. Buitenhuis, J.; Förster, S. *J. Chem. Phys.* **1997**, *107*, 262-272.

27. Hawker, C.J.; Farrington, P.J.; Mackay, M.E.; Wooley, K.L.; Fréchet, J.M.J. *J. Am. Chem. Soc.* **1995**, *117*, 4409-4410.

28. Bosman, A.W.; Vestberg, R.; Heumann, A.; Fréchet, J.M.J.; Hawker, C.J. *J. Am. Chem. Soc.* **2003**, *125*, 715-728.

29. Hecht, S.; Vladimirov, N.; Fréchet, J.M.J. *J. Am. Chem. Soc.* **2001**, *123*, 18-25.

30. Kovář, M.; Strohalm, J.; Etrych, T.; Ulbrich, K.; Říhová, B. *Bioconjugate Chem.* **2002**, *13*, 206-215.
31. Fichter, K.M.; Zhang, L.; Kiick, K.L.; Reineke, T.M. *Bioconjugate Chem.* **2007** ASAP
32. Heyes, C.D.; Groll, J.; Möller, M.; Nienhaus, G.U. *Mol. Biosyst.* **2007**, *3*, 419-430.
33. Sofia, S.J.; Premnath, V.; Merrill, E.W. *Macromolecules* **1998**, *31*, 5059-5070.
34. Xue, L.; Agarwal, U.S.; Lemstra, P.J. *Macromolecules* **2005**, *38*, 8825-8832.
35. Hedrick, J.L.; Magbitang, T.; Connor, E.F.; Glauser, T.; Volksen, W.; Hawker, C.J.; Lee, V.Y.; Miller, R.D. *Chem. Eur. J.* **2002**, *8*, 3309-3319.
36. Kennedy, J.P.; Jacob, S. *Acc. Chem. Res.* **1998**, *31*, 835-841.
37. Hadjichristidis, N.; Pitsikalis, M.: Pispas, S.; Iatrou, H. *Chem. Rev.* **2001**, *101*, 3747-3792.
38. Matthews, O.A.; Shipway, A.N.; Stoddart, J.F. *Prog. Polym. Sci.* **1998**, *23*, 1-56.
39. Zhang, X.; Xia, J.; Matyjaszewski, K. *Macromolecules* **2000**, *33*, 2340-2345.
40. Funke, W.; Okay, O.; Joos-Müller, B. *Adv. Polym. Sci.* **1998**, *136*, 139-234.
41. Gao, H.; Matyjaszewski, K. *Macromolecules* **2006**, *39*, 3154-3160.
42. Haddleton, D.M.; Waterson, C. *Macromolecules* **1999**, *32*, 8732-3739.
43. Stenzel-Rosenbaum, M.H.; Davis, T.P.; Chen, V.; Fane, A.G. *Macromolecules* **2001**, *34*, 5433-5438.
44. Jankova, K.; Bednarek, M.; Hvilsted, S. *J. Polym. Sci., Part A, Polym. Chem.* **2005,** *43*, 3748-3759.
45. Stenzel, M.H.; Davis, T.P. *J. Polym. Sci., Part A, Polym. Chem.* **2002,** *40*, 4498-4512.
46. Kakuchi, T.; Narumi, A.; Matsuda, T.; Miura, Y.; Sugimoto, N.; Satoh, T.; Kaga, H. *Macromolecules* **2003**, *36*, 3914-3920.
47. Ohno, K.; Wong, B.; Haddleton, D.M. *J. Polym. Sci. Part A, Polym. Chem.* **2001**, *39*, 2206-2214.
48. Jacob, S.; Majoros, I.; Kennedy, J.P. *Macromolecules* **1996**, *29*, 8631-8641.
49. Shim, J.S.; Kennedy, J.P. *Polym. Bull.* **2000**, *44*, 493-499.
50. Ueda, J.; Kamigaito, M.; Sawamoto, M. *Macromolecules* **1998**, *31*, 6762-6768.
51. Angot, S.; Murthy, K.S.; Taton, D.; Gnanou, Y. *Macromolecules* **1998**, *31*, 7218-7225.
52. Angot, S.; Murthy, K.S.; Taton, D.; Gnanou, Y. *Macromolecules* **2000**, *33*, 7261-7274.
53. Gnanou, Y.; Taton, D. Macromol. Symp. **2001**, *174*, 333-341.
54. Matyjaszewski, K.; Qin, S.; Boyce, J.R.; Shirvanyants, D.; Sheiko, S.S. *Macromolecules* **2003**, *36*, 1843-1849.
55. Heise, A.; Diamanti, S.; Hedrick, J.L.; Frank, C.W.; Miller, R.D. *Macromolecules* **2001**, *34*, 3798-3801.
56. Cameron, N.S.; Corbierre, M.K.; Eisenberg, A. *Can. J. Chem.* **1999**, *77*, 1311-1326.
57. Lodge, T.P. *Macromol. Chem. Phys.* **2003**, *204*, 265-273.
58. Cui, H.; Chen, Z.; Wooley, K.L.; Pochan, D.J. *Macromolecules* **2006**, *39*, 6599-6607.
59. Pochan, D.J.; Chen, Z.; Cui, H.; Hales, K.; Qi, K.; Wooley, K.L. *Science* **2004**, *306*, 94-97.
60. Cornelissen, J.; Fischer, M.; Sommerdijk, N.; Nolte, R.J.M. *Science* **1998**, *280*, 1427-1430.

61. Lodge, T.P.; Hillmyer, M.A.; Zhou, Z.; Talmon, Y. *Macromolecules* **2004**, *37*, 6680-6682.
62. Raez, J.; Manners, I.; Winnik, M.A. *J. Am. Chem. Soc.* **2002**, *124*, 10381-10395.
63. Kubowicz, S.; Baussard, J.-F.; Lutz, J.-F.; Thünemann, A.F.; von Berlepsch, H.; Laschewsky, A. *Angew. Chem. Int. Ed.* **2005**, *44*, 5562-5265.
64. Yonetake, K.; Nakayama, T.; Ueda, M. *J. Mater. Chem.* **2001**, *11*, 761-767.
65. Ma, Q.; Wooley, K.L. *J. Polym. Sci. Part A: Polym. Chem.* **2000**, *38*, 4805-4820.
66. Böhmer, V.; Shivanyuk, A. In: Mandolini, L.; Ungaro, R., editors. Calixarenes in Action. London: Imperial College Press, 2000. p. 225.
67. Fransen, J.R.; Dutton, P.J. *Can. J. Chem.* **1995**, *73*, 2217-2223.
68. Lukin, O.; Shivanyuk, A.; Pirozhenko, V.V.; Tsymbal, I.F.; Kalchenko, V.I. *J. Org. Chem.* **1998**, *63*, 9510-9516.
69. Högberg, A.G.S. *J. Am. Chem. Soc.* **1980**, *102*, 6046-6050.
70. Abis, L.; Dalcanale, E.; Du vosel, A.; Spera, S. *J. Org. Chem.* **1988**, *53*, 5475-5479.
71. Zhang, Y.; Kim, C.D.; Coppens, P. *Chem. Commun*. **2000**, 2299-2300.
72. Nissinen, M.; Wegelius, E.; Falábu, D.; Rissanen, K. *Cryst. Eng. Commun.* **2000**, *2*, 151-153.
73. Treat, N.D.; Ayres, N.; Boyes, S.G.; Brittain, W.J. *Macromolecules* **2006**, *39*, 26-29.
74. Matyjaszewski, K.; Wang, J.L.; Grimaud, T.; Shipp, D.A. *Macromolecules* **1998**, *31*, 1527-1534.
75. Nanda, A.K.; Matyjaszewski, K. *Macromolecules* **2003**, *36*, 599-604.
76. Matyjaszewski, K.; Shipp, D.A.; Wang, J.L.; Grimaud, T.; Patten, T.E. *Macromolecules* **1998**, *31*, 6836-6840.
77. Haddleton, D.M.; Crossman, M.C.; Dana, B.H.; Duncalf, D.J.; Heming, A.M.; Kukulj, D.; Shooter, A.J. *Macromolecules* **1999**, *32*, 2110-2119.
78. Matyjaszewski, K.; Göbelt, B.; Paik, H.; Horwitz, C.P. *Macromolecules* **2001**, *34*, 430-440.
79. Kickelbick, G.; Reinöhl, U.; Ertel, T.S.; Bertagnolli, H.; Matyjaszewski, K. *ACS Symp. Ser.* **2000**, *768*, 211-222.
80. Xia, J.; Matyjaszewski, K. *Macromolecules* **1997**, *30*, 7697-7700.
81. Matyjaszewski, K.; Xia, J. *Chem. Rev.* **2001**, *101*, 2921-2990.
82. Sumerlin, B.S.; Neugebauer, D.; Matyjaszewski, K. *Macromolecules* **2005**, *38*, 702-708.
83. Heise, A.; Hedrick, J.L.; Trollsås, M.; Miller, R.D.; Frank, C.W. *Macromolecules* **1999**, *32*, 231-234.
84. Bosman, A.W.; Bruining, M.J.; Kooijman, H.; Spek, A.L.; Janssen, R.A.J.; Meijer, E.W. *J. Am. Chem. Soc.* **1998**, *120*, 8547-8548.
85. Heise, A.; Nguyen, C.; Malek, R.; Hedrick, J.L.; Frank, C.W.; Miller, R.D. *Macromolecules* **2000**, *33*, 2346-2354.
86. Shen, Z.; Chen, Y.; Barriau, E.; Frey, H. *Macromol. Chem. Phys.* **2006**, *207*, 57-64.
87. Lepoittevin, B.; Matmour, R.; Francis, R.; Taton, D.; Gnanou, Y. *Macromolecules* **2005**, *38*, 3120-3128.
88. Matyjaszewski, K.; Qin, S.; Boyce, J.R.; Shirvanyants, D.; Sheiko, S.S. *Macromolecules* **2003**, *36*, 1843-1849.
89. Schaefgen, J.R.; Flory, P.J. *J. Am. Chem. Soc.* **1948**, *70*, 2709-2718.
90. Shipp, D.A.; Yu, X. *J. Polym. Sci. Part A: Polym. Chem.* **2004**, *42*, 5548-5558.
91. Queffelec, J.; Gaynor, S.G.; Matyjaszewski, K. *Macromolecules* **2000**, *33*, 8629-8639.

92. Burguière, C.; Chassenieux, C.; Charleux, B. *Polymer* **2003**, *44*, 509-518.
93. Kim, K.H.; Cui, G.H.; Lim, H.J.; Huh, J.; Ahn, C.H.; Jo, W.H. *Macromol. Chem. Phys.* **2004**, *205*, 1684-1692.
94. Whittaker, M.R.; Monteiro, M.J. *Langmuir* **2006**, *22*, 9746-9752.
95. Taton, D.; Cloutet, E.; Gnanou, Y. *Macromol. Chem. Phys.* **1998**, *199*, 2501-2510.
96. Yang, Z.; Liu, J.; Huang, Z.; Shi, W. *Eur. Polym. J.* **2007**, *43*, 2298-2307.
97. Kjøniksen, A-L; Laukkanen, A.; Galant, C.; Knudsen, K.D.; Tenhu, H.; Nyström, B. *Macromolecules* **2005**, *38*, 948-960.
98. Korobko, A.V.; Jesse, W.; Lapp, A.; Egelhaaf, S.U.; van der Maarel, J.R.C. *J. Chem. Phys.* **2005**, *122*, 024902.
99. Park, S.Y.; Han, B.R.; Na, K.M.; Han, D.K.; Kim, S.C. *Macromolecules* **2003**, *36*, 4115-4124.
100. Peters, R. in: Brown, W., editor. Dynamic Light Scattering: The Method and Some Applications. Oxford: Clarendon Press, 1993, p.149.
101. Schillén, K.; Brown, W.; Johnsen, R.M. *Macromolecules* **1994**, *27*, 4825-4832.
102. Jørgensen, E.B.; Hvidt, S.; Brown, W.; Schillén, K. M*acromolecules* **1997**, *30*, 2355-2364.
103. Rager, T.; Meyer, W.H.; Wegner, G.; Winnik, M.A. *Macromolecules* **1997**, *30*, 4911-4919.
104. Selb, J.; Gallot, Y. *Makromol. Chem.* **1980**, *181*, 809-822.
105. Kratochvil, P. in: Huglin, M.B., editor. Light Scattering from Polymer Solutions, London: Academic Press, 1972, p. 333.
106. Pedersen, J.S. *Adv.Colloid Interface Sci.* **1997**, *70*, 171-210.
107. Savin, G.; Burchard, W. *Macromolecules* **2004**, *37*, 3005-3017.
108. Burchard, W. *Macromolecules* **2004**, *37*, 3841-3849.
109. Goldstein, M. *J. Chem. Phys.* **1953**, *21*, 1255-1258.
110. Yoshizaki, T.; Yamakawa, H. M*acromolecules* **1980**, *13*, 1518-1525.
111. Pedersen, J.S.; Schurtenberger, P. M*acromolecules* **1996**, *29*, 7602-7612.
112. Zhang, L.; Eisenberg, A. *J. Am. Chem. Soc.* **1996**, *118*, 3168-3181.
113. Antoun, S.; Gohy, J.-F., Jérôme, R. *Polymer* **2001**, *42*, 3641-3648.
114. Pergushov, D.V.; Remizova, E.V.; Gradzielski, M.; Lindner, P.; Feldthusen, J.; Zezin, A.B.; Müller, A.H.E.; Kabanov, V.A. *Polymer* **2004**, *45*, 367-378.
115. Geng, Y.; Ahmed, F.; Bhasin, N.; Discher, D.E. *J. Phys. Chem. B* **2005**, *109*, 3772-3779.
116. Netz, R.R. *Europhys. Lett.* **1999**, *47*, 391-397.
117. Teng, J.; Zubarev, E.R. *J. Am. Chem. Soc.* **2003**, *125*, 11840-11841.
118. Zhang, L.; Eisenberg, A. *Macromolecules* **1996**, *29*, 8805-8815.
119. Förster, S.; Zisenis, M.; Wenz, E.; Antonietti, M. *J. Chem. Phys.* **1996**, *104*, 9956-9970.
120. Schuch, H.; Kligler, J.; Rossmanith, P.; Frechen, T.; Gerst, M.; Feldthusen, J.; Müller, A.H.E. *Macromolecules* **2000**, *33*, 1734-1740.
121. Antonietti, M.; Bremser, W.; Schmidt, M. *Macromolecules* **1990**, *23*, 3796-3805.
122. Qin, A.; Tian, M.; Ramireddy, C.; Webber, S.E.; Munk, P.; Tuzar, Z. *Macromolecules* **1994**, *27*, 120-126.
123. Dalhaimer, P.; Engler, A.J.; Parthasarathy, R.; Discher, D.E. *Biomacromolecules* **2004**, *5*, 1714-1719.

124. Vriezema, D.M.; Aragonès, M.C.; Elemans, J.A.A.; Cornelissen, J.J.L.; Rowan, A.E.; Nolte, R.J.M. *Chem. Rev.* **2005**, *105*, 1445-1490

125. Tang, J.X.; Janmey, P.A. *J. Biol. Chem.* **1996**, *271*, 8556-8563.

126. Frieden, C. *Ann. Rev. Biophys. Biophys. Chem.* **1985**, *14*, 189-210.